Nanotechnology Perceptions
ISSN 1660-6795
www.nano-ntp.com

Formulation and Evaluation of Niosomes of Fortified Bacoside: A Rich Fraction from Bacopa Monnieri for Memory Enhancement

Shweta Babasaheb Dighe[1], Mahendra Singh Ranawat[2]

[1]*Research Scholar, Department of Pharmacy, Bhupal Nobles' University, Udaipur, Rajasthan, India,*
[2]*Department of Pharmacy, Bhupal Nobles' University, Udaipur, Rajasthan, India*

The triterpenoid saponins, bacosides, and bacoside A are the main active ingredients of Bacopa monnieri that have been shown to improve intelligence or cognition. Bacoside A's low aqueous solubility and blood brain barrier (BBB) restriction are the two factors that limit its bioavailability and clinical efficacy for treating neurodegenerative diseases. Colostrum from cows enhances the cognitive benefits of Bacoside A. In order to deliver Bacopa monnieri 's fortified Bacoside A fraction (Fort-BAF) with enhanced oral bioavailability for possible memory-enhancing activity, the goal of this study was to create and assess the best niosomal formulation. Niosomes were created using the thin-film hydration method, and the hydration volume, cholesterol, and span 60 were the main variables that were optimised using a Box-Behnken Design (BBD) with Response Surface Methodology (RSM). The stability and compatibility of Fort-BAF with other formulation ingredients were validated by preformulation studies. Fort-BAF (BN9)'s optimal niosomal formulation was made and described. An in vivo biological evaluation and in vitro release were conducted to investigate the memory-enhancing properties of the optimised niosomal formulation (BN9) in comparison to the Bacoside A rich fraction. With a favourable zeta potential of -28.5 mV, a small particle size of 121.7±3.22 nm, and a high entrapment efficiency of 87.56%, the optimised BN9 showed promising properties that indicated stability and efficacy. According to the Higuchi model, in vitro drug release studies showed that 75.42% of the drug was released in an hour. The niosomes' spherical shape and porous structure were validated by SEM and TEM analyses. According to stability tests, the formulation holds up well over a three-month period. According to in-vivo

research findings, BN9 may improve learning and memory. The findings imply that niosomes can greatly improve the Fort-BAF's stability and bioavailability. The potential of niosomal formulations as a viable method for delivering Bacopa monnieri 's Fort-BAF to the brain in neuroprotection and cognitive enhancement treatments is highlighted by this study.

Keywords: Fortified Bacoside A fraction, Niosomes, Thin-Film Hydration Method, Response Surface Methodology (RSM), memory enhancement activity.

1. Introduction

The Bacopa monnieri (L.) Pennell (Brahmi), a traditional medicine used as a brain or nerve tonic across the world for generations, [1] as an anti-inflammatory, cognitive or memory enhancing (medhyarasayana-rejuvenation of intellect or cognition) [2] and antiepileptic agent for treating neurodegenerative diseases such as Dementia, Alzheimer's disease (AD), epilepsy, anxiety, and stress [3,4]. Number of reasons has been attributed to cause neurodegenerative diseases mainly memory / cognitive dysfunction. Major among these are degradation of the neurotransmitter acetylcholine by the acetyl cholinesterase (AChE) enzyme [5], and β-amyloid protein in the brain [6],□-aggregation of produced by beta-site amyloid precursor protein cleaving enzyme 1 (BACE1) [7]. Many research works proved that the neuroprotective effect of Brahmi is mainly caused by inhibiting β-amyloid protein.Chemical characterization studies on Brahmi revealed the major active constituents are the triterpenoid saponins, bacosides, Bacoside A, responsible for above effects. The bioactive constituent, bacoside A, present in the B. monnieri extract (BME) - treated rat serum and could directly or indirectly interact with the neurotransmitter systems to improve memory and learning ability. [8] Bacoside A, a vital neuroprotective constituent, is composed of four constituents viz., bacoside A3, bacopaside II, jujubogenin isomer of bacopasaponin C (bacopaside X) and bacopasaponin C (Table 1). Bacosides present in B. monnieri are commonly nonpolar glycosides [9].

Table 1. Constituents of Bacoside A in Bacopa monnieri

Name	Aglycone	Sugar Moiety
Bacoside A3	Jujubogenin	3-β-[O-β-D-glucopyranosyl(1→3)-O-[α-L-arabinofuranosyl(1→2)-O-β-Dglucopyranosyl)oxy]
Bacopaside II	Pseudojujubogenin	3-O-[α-L-arabinofuranosyl-(1→2)]-β-D-glucopyranosyl-(1→3) β-D-glucopyranoside
Bacopaside X (Jujubogenin isomer of Bacopasaponin C)	Jujubogenin	3-O-[α-L-arabinofuranosyl-(1→2)]-β-D-glucopyranosyl-(1→3)-α-L-arabinopyranoside
Bacopasaponin C	Pseudojujubogenin	3-O-[β-D-glucopyranosyl(1→3){α-L-arabinofuranosyl(1→2)} α-L-arabinopyranoside

[These saponins contain three sugar units with either jujubogenin or pseudojujubogenin as their aglycone subunits. Names of sugar units are listed as in the original literature] [10-13]

Neuroprotective mechanism of Bacoside A

In a recent study, Bacoside-A protect the brain against oxidative damage and age-related cognitive deterioration with multifaceted mechanisms of action [14, 15], such as, exerted

significant inhibitory effects upon cytotoxicity, fibrillation, and particularly membrane interactions of amyloid-beta (1-42) (Aβ42), the peptide playing a prominent role in memory dysfunction, AD progression and toxicity [16]. In addition, bacosides prevent Aß aggregation and formation of fibrils [17], as well as protect neurons against Aβ-induced toxicity [18]. Thus, Bacoside A established as an important nutraceutical against neurodegenerative diseases. However, the two factors hamper the bioavailability of Bacoside A, first main hurdle is that its oral administration has been limited due to its low aqueous solubility. And second, the bioavailability as well as binding of bacosides to the neuroreceptors is controlled by the Blood Brain Barrier (BBB), which restricts drug efficacy. However, Nanoformulation of Bacoside A easily resolves the BBB restriction and carries a promising role in future therapies [19].

Neuroprotective and cognitive enhancing effects of Bovine colostrum

Colostrum is the first milk produced by mammals for their young. It plays an important role in protection and development by providing various antibodies, growth factors and nutrients, and has been used for various diseases in many countries. Sung Eun Kim et al [20] suggested that bovine colostrum improved short-term memory following hippocampal hemorrhage in rats which shows colostrum may have a beneficial role in recovering brain function. Schuster et al [21] reported that colostrinin, a class of proline-rich polypeptides derived from colostrum, had a protective effect on neuroblastoma cells by reducing fibril formation and cell death induced by beta-amyloid. Marta Sochocka1 et al [22] indicated PRP as a potential target for future treatments in neuroinflammatory diseases like AD. Popik et al [23] reported that colostrinin, one of the polypeptides derived from colostrum, facilitated the acquisition and retrieval of spatial memory and long-term memory in aged rats, and Bilikiewicz and Gaus[24] reported that colostrinin retarded the progression of Alzheimer's disease. Liposomal technology has been used to preserve bovine colostrum and increase its bioavailability for human health [25, 26]. In the present study, bovine colostrums is used for fortification of bacoside A fraction of Bacopa monnieri. Bovine colostrum have health benefits that complement the cognitive enhancing properties of Bacoside A.

Strengths of Niosomes in Drug Delivery

Despite of promising therapeutic properties, biomolecules Bacoside A, having low water solubility, which in turn resulted in their poor bioavailability and less efficacy. Development of nanocarriers has opened new avenues for the delivery of therapeutics of various pharmacological activities, to improve their stability, drug efficacy and pharmacokinetic profiles, and targeting properties [27].Hence, researchers tried to enhance water solubility and bioavailability of Bacoside A by loading them in biodegradable polymeric nanoparticles. Jose et al.[28] recently demonstrated the high efficiency of bacoside A-loaded PLGA nanoparticles in delivering bacoside A into the brain, crossing the BBB. Vitthal KU, et al.,[29] developed Bacoside loaded Solid lipid nanoparticles (SLN) by micro emulsion probe sonicator method. Kumar R, et al., [30] developed Bacoside rich extract loaded Solid lipid nanoparticles (SLN), as a new approach for CNS targeting and nootropic effect in the treatment of neurodegenerative diseases.Numerous researches have examined vesicular systems at the nanoscale, including liposomes and niosomes, a more recent class of vesicular nanocarriers. The lipophilic and hydrophilic bioactive materials in the self-assembled vesicle

which are made of non-ionic surfactants along with cholesterol or other amphiphilic molecules are transported across several membranes by the niosomes. Niosomes share structural similarity with liposomes while overcoming limitations associated with stability, sterilization, and large-scale production of liposomes. Niosomes are thought to be more chemically and physically stable than liposomes [31]. Moreover, niosomes provide additional advantages compared to other micro- and nano-delivery systems, which are low-cost manufacturing, ease of scale-up production, possess higher stability and longer shelf-life. Niosomes are undoubtedly a promising and cutting-edge drug delivery technology which can effectively improve the delivery of important phytochemical compounds at the site of action by facilitating the crossing of blood brain barrier (BBB).

Particularly, triterpenoid saponins called Bacoside A have been considered to be the major bioactive constituents responsible for the memory enhancing effects of B. monnieri. Colostrum is the pre-milk fluid produced by mammals during the first 72 hours after birth. The cow colostrum contains a proline rich polypeptide (PRP), named Colostrinin (CLN) which improves learning and memory in rats, delays the progression of dementia and loss of long term memory in aging animals [32]. This study aimed at developing and optimizing a Niosomes of Fort-BAF from Bacopa monnieri to promote targeted drug delivery with enhanced CNS bioavailability. Fort-BAF -loaded niosomes were prepared by thin film hydration technique. The optimized formulation was characterized and then subjected to pharmacological evaluation for memory enhancing activity by using behavioral models like Morris Water Maze and Y-Maze.

2. MATERIAL AND METHODS:

MATERIAL:

The fresh aerial parts of Bacopa monnieri were sourced from Wagh Nursery, Manjari, Pune. Bacoside A, used as a marker compound, was generously provided by Manikarnika Ayurveda, Pune. Bovine colostrum (Piyush Ghan) purchased from Inlife health care. Cholesterol (97% extra pure) and Span 60 (Sorbitan monostearate) were obtained from LOBA Chemie. Analytical-grade chloroform, ethanol and methanol were also procured from LOBA Chemie.

METHOD:

2.1. Plant collection, extraction, isolation and characterization Bacoside A rich fraction from Bacopa monnieri :[33]

The sample of fresh aerial part of Bacopa monnieri (Plantaginaceae) was collected from Wagh Nursery Manjari, Pune (Lat. 18.5235° Lng. 73.9854°) and was authenticated by Mr. D.L.Shirodkar, Botanist, Botanical Survey of India, Pune by comparing morphological features with the Voucher specimen number (SBDBM-1) and Ref. No. (BSI/WRC/lden. Cer./2022/3003220017319 HT). The Bacoside A marker was a generous gift from Manikarnika Ayurveda Pimpri-Chinchwad, Pune. All the other chemicals were of analytical grade and were used as received.

Shade dried aerial part of plant used and was extracted utilizing 70% Methanol under reflux

for 4 hrs. The collected plant extract was concentrated under vacuum and the concentrated extract was dissolved in 1L of n-butanol and three times washed with water. The n-butanol layer was evaporated and dried under vacuum to obtain a thick paste. The ethyl acetate extractives were removed from the thick paste under reflux and obtained residue was concentrated. Above residue then subjected to column chromatography over silica gel using eluants with a slow gradient of increasing polarity starting from CHCl3 –MeOH-H2O for isolation of Bacoside A rich fraction. The fractions that were eluted with CHCl3/MeOH 8:2 yielded Bacoside A rich fraction (a mixture of four triglycosidic saponins).

Identification of bacosides (triterpenoid saponins) done by Preliminary phytochemical analysis and quantitative determination of saponin content was found to be 21.5 %.The isolated fraction was found to be in compliance with the reported parameters. UV-scan of Bacoside A rich fraction in methanol showed λmax 273 nm. FTIR study showed comparable characteristic bands at 3431, 2940, 2855, 1638, 1451, 1078 cm−1 in Bacoside A rich fraction as that of marker. DSC, UV spectroscopy, Thin Layer Chromatography (TLC), characterized the extracts and confirmed the identity of Bacoside A. HPLC results confirmed the standardized isolation of Bacoside A rich fraction. The LC-ESI-MS analysis identified major triterpenoid saponins in the isolated Bacoside A fraction by showing characteristic m/z 455.4 for jujubogenin glycosides (bacoside A3 and bacopaside X) and also characteristic m/z 473.5 for pseudojujubogenin glycosides (bacopaside II and bacopasaponin C).Overall, the study confirmed the presence of Bacoside A, the key active compounds in the isolated fraction of Bacopa monnieri . The isolated Bacoside A fraction was used to formulate the niosome formulation.

2.2. Niosomes preparation:

2.2.1. Method: Thin Film hydration method [34]

Based on the results of previous research works our fortified Bacoside A rich fraction(Fort-BAF) loaded niosomes were prepared using thin film hydration method [35] with slight modifications. Definite weights of Bacoside A rich fraction +Bovine colostrum (200mg), surfactant (span 60) and cholesterol were dissolved in chloroform: Methanol (10ml) in a round bottom flask. The Solvent was evaporated at 40 °C under reduced pressure using rotary evaporator at 60 rpm. The dried thin film was hydrated at temperature 55 °C with aqueous phase. The prepared niosomal suspension after hydration was subjected to bath sonication for 10 min. that leads to formation of small unilamellar vesicles.

Then the drug loaded niosomal suspension were lyophilized using a freeze dryer (Germany) for the convenience of storage, transport and dosing. Each sample was rapidly precooled at -25˚C, and lyophilized for 24 hr. at a temperature of -50˚C and a vacuum of 3 mmHg.

2.2.2. Optimization of Fort-BAF loaded Niosomes by Design of Experiment (DOE)

In this study, a Response Surface Methodology (RSM) known as Box Behnken Design was utilized with Design Expert® software (Version 13.0). The Box Behnken Design involved three independent variables: the amount of Span 60 (mg) (A), Cholesterol (%) (B),and the hydration volume (ml) (C). The dependent variables examined were entrapment efficiency (%), zeta potential (mv) and particle size (nm).The Box Behnken Design included factorial points, a center point, and axial points, resulting in a total of 13 experimental runs. The

details of the independent variables, their coded levels, and the Box Behnken Design scheme matrix are provided in the accompanying table.

Table 2: Box-Behnken design for Fort-BAF loaded niosomes depiting Independent variables and their level of variation

Independent Variables	Unit	Low Actual	High Actual
Span 60 of (A)	mg	60	120
Cholesterol (B)	mg	10	70
Hydration volume (C)	ml	5	10

Table 3: Model fitting with EE, zeta potential and particle size of vesicles for niosomes

Response	Name	Units	Analysis	Minimum	Maximum	Mean	Std. Dev.	C.V%	Model
Y1	EE	%	Polynomial	54	87.56	64.26	5.97	9.29	2F1
Y2	Zeta potential	mv	Polynomial	-11.3	-28.93	19.45	1.99	10.24	Quadratic
Y3	Particle Size	nm	Polynomial	121.7	265	192.75	13.15	6.82	Quadratic

Table 4: DOE Suggested and experimental batches of niosome formulation

Formulation Code	Span 60 (mg)	Cholesterol (mg)	Hydration volume (ml)	Chloroform :Methanol (ml)	Conc. of Bacoside A +Bovine colostrum(mg)
BN1	60	10	7.5	1:1	1:1
BN 2	120	70	7.5	1:1	1:1
BN 3	120	40	5	1:1	1:1
BN 4	60	40	5	1:1	1:1
BN 5	120	10	7.5	1:1	1:1
BN 6	90	70	5	1:1	1:1
BN 7	90	10	10	1:1	1:1
BN 8	60	70	7.5	1:1	1:1
BN 9	60	40	10	1:1	1:1
BN 10	90	40	7.5	1:1	1:1
BN 11	90	10	5	1:1	1:1
BN 12	90	70	10	1:1	1:1
BN 13	120	40	10	1:1	1:1

2.3. PREFORMULATION STUDY

2.3.1. Melting point determination:[36]

The lyophilized powder of Bacoside A rich fraction and Bovine colostrum melting point was determined using the Capillary method and a thieles tube melting apparatus. A glass capillary tube is filled with drug powder and one end is sealed. This capillary is tied with a thermometer and placed in a thieles tube containing liquid paraffin so that the drug-containing end is submerged in the paraffin. Heat is applied to the Thieles tube using a burner, and the temperature at which the drug melts is recorded. Readings are taken in triplicate.

2.3.2. Determination of lambda max:[37]

The Bacoside A rich fraction and Bovine colostrum lyophilized powder sample was prepared by dissolving 10 mg of drug in 10 ml phosphate buffer solution pH 7.4 respectively. The samples of the standard solution were scanned between 200-400 nm regions on Jasco UV spectrophotometer (Jasco v-630).

2.3.3. Preparation of calibration curve: [38]

Standard stock solution was prepared by taking 50 mg lyophilized powder in 50 ml of Phosphate buffer pH 7.4 (1000µg/ml). The stock solution scanned in the range 200-400 nm by UV spectrophotometer (Jasco v-630). The solution showed maximum absorbance at 273 nm. From 1000µg/ml, diluted 10 ml to 100ml (100 µg/ml), from this solution (10-60 µg/mL) dilutions prepared. Absorbance was taken at 273 nm. Using Phosphate buffer pH 7.4 as a blank. The absorbance v/s concentration graph is plotted.

2.3.4. Determination of solubility: [39]

The solubility of Bacoside A rich fraction and Bovine colostrum was performed in Methanol, ethanol, distilled water, chloroform, phosphate buffer pH 7.4, Phosphate buffer pH 6.8, Acidic buffer pH 1.2(50ml) were taken in different100 ml conical flask & 50 mg of Bacoside A rich fraction and Bovine colostrum were added in it. The conical flask was stirred for 24 hrs. On mechanical shaker at 150 RPM. After 24 hrs the flask was removed solutions were filtered and absorbance was measured at 273 nm.

2.3.5. Fourier-transform infrared spectroscopy analysis: [40]

The FTIR spectra of Bacoside A rich fraction, Bacoside A rich fraction +Bovine colostrums and Physical mixture (Bacoside A rich fraction +Bovine colostrum: Span 60: Cholesterol) were recorded and interpreted for the possible chemical interactions. The transparent pellets of these samples were prepared by mixing each of these components with potassium bromide, and FTIR spectra were recorded in the region of 4000–400 cm-1 (Jasco FTIR-4600).

2.3.6. Differential Scanning Calorimetry: [41]

The thermal behavior of Bacoside A rich fraction, Bacoside A rich fraction +Bovine colostrums and Physical mixture (Bacoside A rich fraction +Bovine colostrum: Span 60: Cholesterol) were studied using DSC (METTLER TOLEDO, SW STARe, and USA). DSC studies were performed to know the physical state of the drug. For the analysis, 2-5 mg of the sample weighed in standard aluminum pans were used and hermetically covered with lead. The heating range was 50- 300°C for a sample with a constantly increasing rate of temperature at 10°C/min under the nitrogen atmosphere (50-60mL/min/). The resulting thermogram of all samples were obtained.

2.3.7. X-ray Diffraction:

X-ray diffraction (XRD) patterns for the samples of Bacoside A rich fraction, Bacoside A rich fraction + Bovine colostrum and physical mixture (Bacoside A rich fraction + Bovine colostrum: Span 60: cholesterol) were compared in the crystallographic investigation using an X-ray diffractometry (XRD) (Bruker D8 Advance) with Cu-K radiation (λ=1.54) at a voltage of 40 kV, 50 mA, at increments of 0.02º from 5º to 100º diffraction angle (2θ) at 1 s/step. Samples were scanned against a zero backdrop.

2.4. Characterization of Fort-BAF loaded Niosomes

Particle size and zeta potential determination: [42]

The 3-5mg of formulation was taken and mixed with distilled water and sonication was kept for 30min. The analysis was performed at a temperature of 25°C. Then same procedure repeated for zeta potential (Horiba,SZ100).

Entrapment efficiency: [43]

The entrapment efficiency of niosomes formulation was determined by centrifugation method, in which10mg in10ml methanol of the prepared niosomal suspension was placed in the Eppendorf for centrifugation (RM-12) at 1000 rpm for 30min after centrifugation, the supernatant liquid was separated, containing the un-entrapped drug, diluted with methanol and analyzed using UV spectrophotometer at 273 nm. By using that absorbance entrapment efficiency(%EE).

% Entrapment Efficiency = (Total drug - Drug in supernatant)/(Total drug)×100

Fourier-transform infrared spectroscopy analysis: [40]

The FTIR spectra of optimized batch (BN9) were recorded and interpreted for the possible chemical interactions. The transparent pellets of these samples were prepared by mixing each of these components with potassium bromide, and FTIR spectra were recorded in the region of 4000–400 cm-1 (Jasco FTIR-4600).

Differential Scanning Calorimetry: [41]

The thermal behavior of optimized batch (BN9) was studied using DSC (METTLER TOLEDO, SW STARe, and USA). DSC studies were performed to know the physical state of the drug. For the analysis, 2-5 mg of the sample weighed in standard aluminum pans were used and hermetically covered with lead. The heating range was 50- 300°C for a sample with a constantly increasing rate of temperature at 10°C/min under the nitrogen atmosphere (50-60mL/min/). The resulting thermogram of sample was obtained.

XRD: [44]

X-ray diffraction pattern of optimized batch (BN9) was measured in the crystallographic investigation using an X-ray diffractometry (XRD) (Bruker D8 Advance) with Cu-K radiation (λ=1.54) at a voltage of 40 kV, 50 mA, at increments of 0.02º from 5º to 100º diffraction angle (2θ) at 1 s/step. Optimized batch (BN9) was scanned against a zero backdrop.

Scanning Electron Microscope (SEM): [45]

Scanning electron microscopy (SEM) (Nova NanoSEM NPEP303), was used to examine the surface morphology, size, and texture of vesicles of optimized batch (BN9) using platinum sputter technique.

Transmission Electron Microscope (TEM): [46]

The surface morphology of the optimized batch BN9 was established by using Transmission Electron Microscopy (TEM) (JEOL, 220FS).Few microliters of diluted solution of optimized batch BN9 was put on 300 mesh copper grid film coated with copper and were air-dried at room temperature. Once it was dried completely, the sample was stained using a 2 % w/v phosphotungstic acid solution removing the excess with a filter paper. Further, the analysis

and images of samples were examined and photographed by using digital micrograph and Soft Imaging Viewer Software.

In Vitro Drug Release study: [47]

The release of drug from provesicular powders was determined in HCl (pH 1.2) and Phosphate buffer solution (PBS), pH 7.4 using a vertical Franz diffusion cell (DBKSrNo-210796). The receptor compartment contained 100 mL dissolution medium maintained at 37.5˚C by means of a thermostatically controlled water bath and magnetic stirring at 50 rpm. Aliquots (1 mL), after 0.25, 0.5, 0.75, 1, 2, 4, 6, 8, 12, 24, 36 and 48 h using a syringe, were filtered through 0.2 mm membrane filter and determined by UV–Vis spectrophotometry (JASCO V-560). Each sample was replaced with fresh medium to maintain sink conditions. Dissolution experiments were carried out in triplicate.

Stability Studies: [48]

Short-term stability analysis of optimized batch (BN9) formulation was performed as per ICH Q1A R2 stability study guidelines. The stability of the optimized batch (BN9) was investigated by storing them at 5±3 °C and 25±2 °C/ 75% relative humidity (RH) for a total of 3 months. Vesicle size, zeta potential and entrapment was evaluated to characterize the stability profile. Visual examination was also done to evaluate any color changes in formulation.

In-vivo Study

Morris water maze Test and Y-maze task. Acute toxicity studies have been already done in previous studies and it was found to be safe up to 2000mg/kg. [49]

Experimental Design

The Institutional Animal Ethical Committee clearance were obtained vide reference 20/ BNCP/IAEC/2021 for the study of memory enhancing activity in Bacoside A rich fraction of Bacopa monnieri .

Swiss male Albino Mice (25-30gm) were procured from Animal House, BNCP. They were acclimatized for laboratory condition for 7 days and randomly divided into five groups each having six animals. The animals were housed under standard laboratory conditions and maintained under a 12-h light- dark cycle and had free access to drinking water and diet for one week. All the protocols in this study were approved by the ethics committee.

For the pharmacological tests, the Bacoside A rich fraction and Optimised Niosomal formulation (BN9) were suspended in double distilled water containing carboxy methylcellulose (1%w/v CMC) in dose of 200mg/kg p.o. The dose was fixed based on earlier studies. Bacoside A rich fraction and Optimised Niosomal formulation (BN9) caused no abnormality or death during the course of treatment.

Drug and Chemicals

Scopolamine was purchased from Sigma Chemicals. Piracetam was purchased from local medical shop.

Grouping of Animals and treatment protocol

Total 30 animals were randomly divided into five different groups, each group containing 6 mice and treated for 18 days. Amnesia mainly induced by using Scopolamine into the mice. Scopolamine (0.4mg/kg) was administered at last three days. Groups are divided as follows.

Group 1: It represented the control group. Vehicle was administered orally for eighteen successive days.

Group 2: It represented amnesia/memory loss induced group (negative control). CMC was administered orally for fifteen successive days followed by Scopolamine (0.4mg/kg i.p.) after 45 min of administration daily from 16th day to 18th day.

Group 3: Piracetam injection was administered i.p. (200mg/kg) for fifteen successive days followed by Scopolamine (0.4mg/kg i.p) after 45 min of administration daily from 16th day to 18th day.

Group 4: Bacoside A rich fraction (200mg/kg) of Bacopa monnieri was administered orally for fifteen successive days followed by Scopolamine (0.4mg/kg i.p.) after 45 min of administration daily from 16th day to 18th day.

Group 5: Optimised Niosomal formulation (BN9) (200mg/kg) was administered orally for fifteen successive days followed by Scopolamine (0.4mg/kg i.p.) after 45 min of administration daily from 16th day to 18th day.

Memory Enhancing Activity:

The pharmacological evaluation of memory enhancing activity was done by using two extroceptive behavioral models, Morris water maze and Y-maze task.

Morris Water Maze: [50,51]

The procedure used was a modification method described by Morris (1984). Mice (25-30g) were trained to find a submerged platform (6.5cmdiameter1cm below surface) in a circular pool (diameter60cm; height30cm) filled with turbidity water (depth19.5cm; 25±1◦C). External visual cues were placed around the pool to facilitate navigation of the animals. The platform was fixed at SW (southwest) direction. Start positions alternated between NE (northeast), SE (southeast), and NW (northwest) direction in a pseudo-random fashion. Each mouse was placed in the water facing the wall of the pool and allowed to swim for 60s to reach the platform. Finding the platform was defined as being able to stay on it for at least 2s; mice that crossed the platform without stopping (jumping immediately back into the water) were left to swim until the termination of the trail. If mouse failed to find the platform in the allotted time, the mouse was manually placed onto the platform manually and assigned as a latency of 60s. All mice were allowed to rest there for 5mts and then performed the next trial immediately. After the last trail, mice were dried with a cloth and then returned to their home cage. Mice performed four consecutive trials per day over a 4-day training period.

The time to reach the target (escape latency) for each mouse was recorded manually. On the last day (day-5) a probe trail was adopted. Each mouse started at NE and had to swim freely for 60 s. memory retention was measured by quantifying the time to reach in the target platform.

Y-Maze Task: [52, 53]

Short-term memory (STM) function was assessed by recording Spontaneous Alternation Behavior (SAB) in a Y-maze according to the procedure described by Hughes (2004). The Y-maze consisted of three arms of equal size, labelled as A, B, and C, respectively. Each arm was 19 cm long, 5 cm wide, and 14.5 cm high and was oriented at an angle of 120° from the other two. Mice were placed within one arm, and the sequence (e.g., CBABCC) and the number of arm entries were recorded manually for each mouse over a five-minute session. Alternation was defined as consecutive entries by a mouse into the three different arms. An arm entry was judged to be completed when the hind paws of the mouse were completely placed in an arm. The arena was cleaned using 70% v/v ethanol between trials so as to avoid olfactory cues. The initial arm of the maze was also changed within mice of the same group in order to avoid bias of arm placement. The parameters measured included number of arm entries, same arm returns (SAR), and alternate arm returns (AAR). Percentage of spontaneous alternation performance (%SAP) was determined using the equation,

$$\%SAP = \frac{\text{Actual Alterations (Total alterations)}}{\text{Total Number of Arm entries-2}} \times 100$$

3. RESULTSAND DISCUSSION

3.1. Preformulation Study:

3.1.1. Determination of melting point

The melting point of Bacoside A rich fraction + Bovine Colostrum was found to be 242℃. Hence, It is in close agreement with the reported value of standard Bacoside A.

3.1.2. Determination of λmax

The solution was scanned on UV spectrophotometer and maximum wavelength (λmax) of the compound was found to be 273 nm. (Fig. 1)

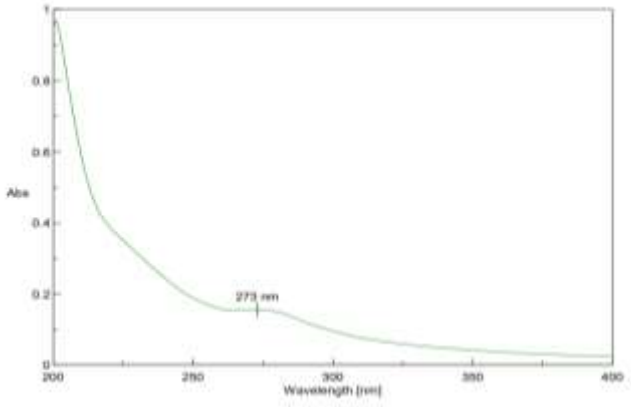

Figure 1: λmax of Bacoside A rich fraction + Bovine Colostrum

3.1.3. Preparation of Calibration Curve

Calibration curve of Bacoside A rich fraction + Bovine Colostrum was prepared to know the straight line equation. Calibration curve along with straight line equation are given in (Fig.2)

Table 5: Absorbance for Bacoside A rich fraction + Bovine Colostrum

Conc. (µg/ml)	Abs.
10	0.048
20	0.094
30	0.135
40	0.174
50	0.212
60	0.254

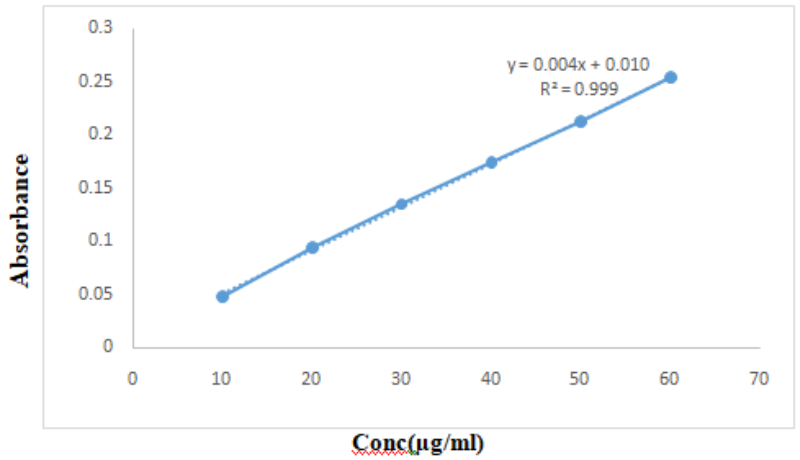

Figure 2: Calibration Curve

3.1.4 Solubility of Bacoside A fraction and Bovine colostrum

After solubility analysis it was established that methanol exhibited the highest solubility, at making it the most effective solvent for dissolving these compounds. Following methanol, ethanol showed a result indicating it is also capable of effectively solubilizing the substances, albeit to a lesser degree. In contrast, the solubility in distilled water was lower, demonstrating moderate solubility in aqueous environments. Chloroform also showed low solubility. Both phosphate buffers at pH 7.4 and pH 6.8 provided relatively good solubility. However, acidic buffer pH 1.2 resulted in the lowest solubility, indicating poor solubility in highly acidic conditions. (Table 6)

Table 6:Solubility of Bacoside A rich fraction + Bovine Colostrum

Medium	Solubility(µg/ml)	Solubility(mg/ml)
Methanol	0.004256	42.56
Ethanol	0.003056	30.56
Distilled water	0.002563	25.63
Chloroform	0.002031	20.31
PhosphatebufferpH7.4	0.002923	29.23
PhosphatebufferpH6.8	0.002412	24.12
Acidic buffer pH 1.2	0.002036	20.36

3.1.5 Fourier Infra –Red Spectroscopy (FTIR):

The FTIR spectra analysis of the Bacoside A rich fraction provides detailed insights into its chemical structure by identifying key functional groups. The O–H stretch for alcohols is observed at 3431.18 cm^{-1}, 3380.96 cm^{-1}, and 3087.14 cm^{-1}, slightly below the reported range of 3500–3200 cm^{-1}, which is typical of hydroxyl groups in complex organic compounds. The O–H stretch for carboxylic acids appears at 2940.42 cm^{-1} and 2855.4cm^{-1}, which is within the expected range of 3300–2500 cm^{-1}, confirming the presence of carboxylic acids. The –C=C– stretch (alkenes) is observed at 1638.80 cm^{-1}, fitting well within the reported range of 1680–1640 cm^{-1}, indicating the presence of alkenes. The C–C stretch (in-ring) at 1451.29 cm^{-1} aligns with the expected range of 1500–1400 cm^{-1}, confirming aromaticity. The C–H stretch for alkanes at 1384.91 cm^{-1} is within the expected range of 1370–1350 cm^{-1}, confirming the presence of alkane groups. Additionally, C–O stretches at 1227.25 cm^{-1} and 1078.74 cm^{-1} fit within the reported range of 1320–1000cm^{-1}, suggesting the presence of esters or ethers. The C–H stretch for aromatic rings is observed at 844.90 cm^{-1}, aligning with the reported range of 900–675 cm^{-1}, confirming the presence of aromatic compounds. Overall, the spectra closely match the reported ranges verifying the molecular components of the Bacoside A rich fraction. (Fig. 3)

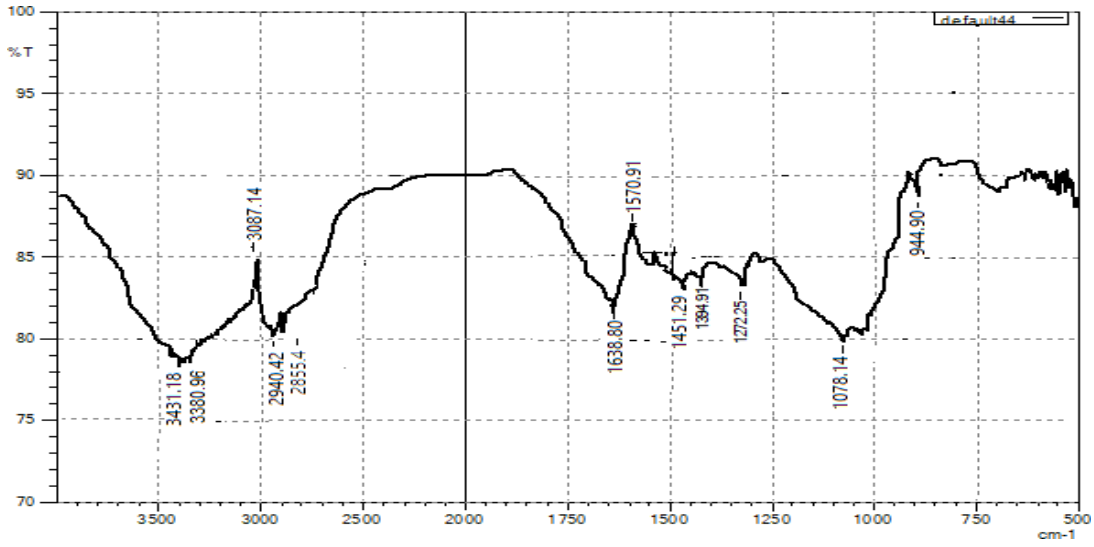

Figure 3: FTIR spectra Bacoside A rich fraction

The FTIR spectra analysis of Bacoside A rich fraction + Bovine Colostrum reveals the presence of key functional groups, confirming their chemical structure. The observed O–H stretch for alcohols appeared at 3430.8 cm^{-1} and 3396.10 cm^{-1}, which is close to the reported range of3500–3200 cm^{-1}, indicating the presence of hydroxyl groups. The O–H stretch for carboxylic acids was noted at 2923.15 cm^{-1} and 2864.4 cm^{-1}, slightly lower than the reported range of 3300–2500 cm^{-1}, which might be due to interactions within the sample matrix. A C=O stretch was observed at 1780 cm^{-1}, fitting well within the reported range of1760–1665 cm^{-1}, suggesting the presence of carbonyl groups. Additionally, the C–C stretch (in-ring) appeared at 1450.8 cm^{-1}, aligning with the expected range of 1500–1400 cm^{-1}, confirming aromaticity. The absence of specific C–H stretching signals for alkanes, typically in the

1370–1350 cm^{-1} range, suggests lower alkane presence, while C–O stretches were found at 1227.25 cm^{-1} and 1210.3 cm^{-1}, within the reported range of 1320–1000 cm^{-1}. Overall result potentially indicating compatibility between the bioactive compounds in Bacoside A rich fraction and Bovine Colostrum. (Fig. 4)

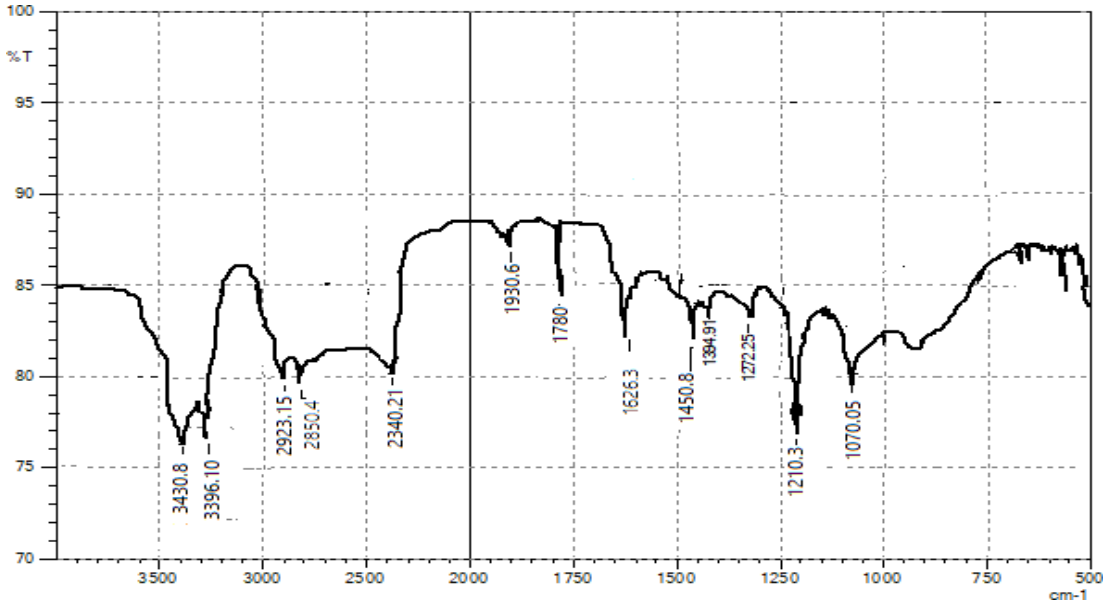

Figure 4:FTIR spectra of Bacoside A rich fraction + Bovine Colostrum

The FTIR spectra of the physical mixture (Bacoside A rich fraction +Bovine colostrum: Span 60: Cholesterol) revealed various characteristic peaks corresponding to key functional groups. Strong broad peak in the region 3450-3400 cm^{-1} indicating O-H stretching vibrations for hydroxyl groups in Bacoside A (being a saponin glycoside), OH groups present in proteins and other components of Colostrum and also in Cholesterol. Sharp peaks around 2942 cm^{-1} representing C-H stretching vibrations for alkyl chains in Span 60 (sorbitan monostearate), steroid ring structure of Cholesterol and hydrocarbon portions of Bacoside A. 1633-1650 cm^{-1} region indicating C=O stretching vibrations from ester groups in Span 60, peptide bonds in Colostrum proteins and carbonyl groups in Bacoside A. Peaks around 1400-1200 cm^{-1} region representing C-O stretching and O-H bending vibrations from glycosidic bonds in Bacoside A, ester linkages in Span 60 and various functional groups in Colostrum proteins. Peaks below 1000 cm^{-1} (Fingerprint region) indicating complex overlapping peaks representing ring breathing modes of steroid nucleus (Cholesterol), sugar ring vibrations from Bacoside A and various skeletal vibrations from all components.

The spectrum showed good preservation of characteristic peaks from all components, suggesting they maintain their chemical integrity in the physical mixture without significant chemical interaction or degradation. This data confirmed the presence of the keyfunctional groups in the physical mixture. (Fig. 5)

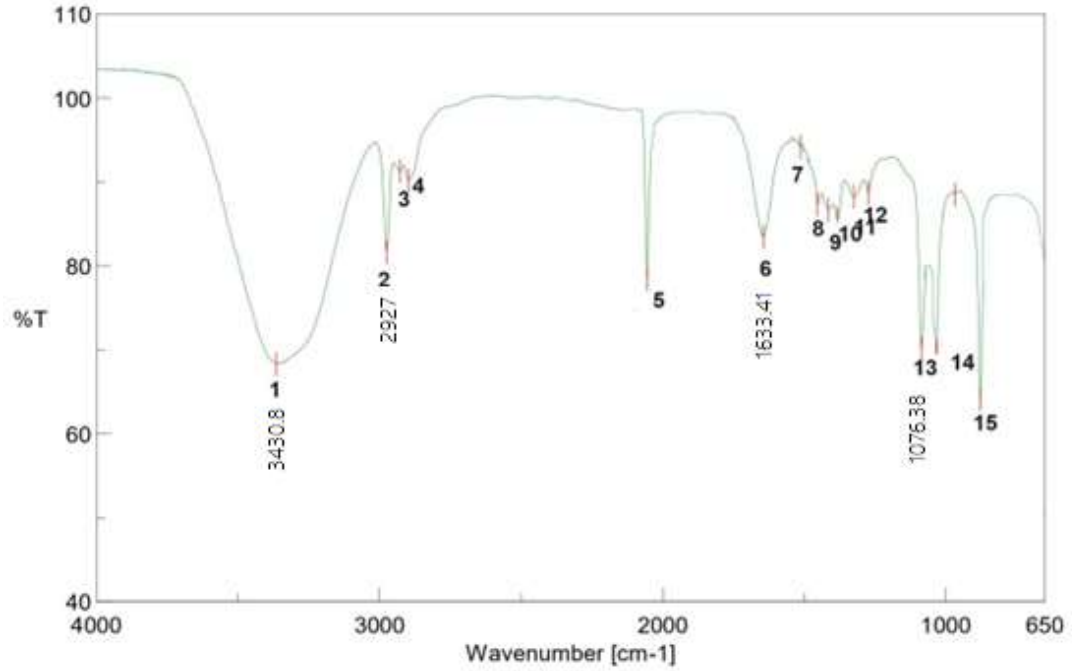

Figure 5: FTIR spectra of Physical Mixture (Bacoside A rich fraction +Bovine colostrum: Span 60: Cholesterol)

3.1.6 Differential Scanning Calorimetry (DSC)

DSC thermogram of Bacoside A rich fraction of Bacopa monnieri can be observed in Fig. 6 below and it showed the peak at 242.10°C.

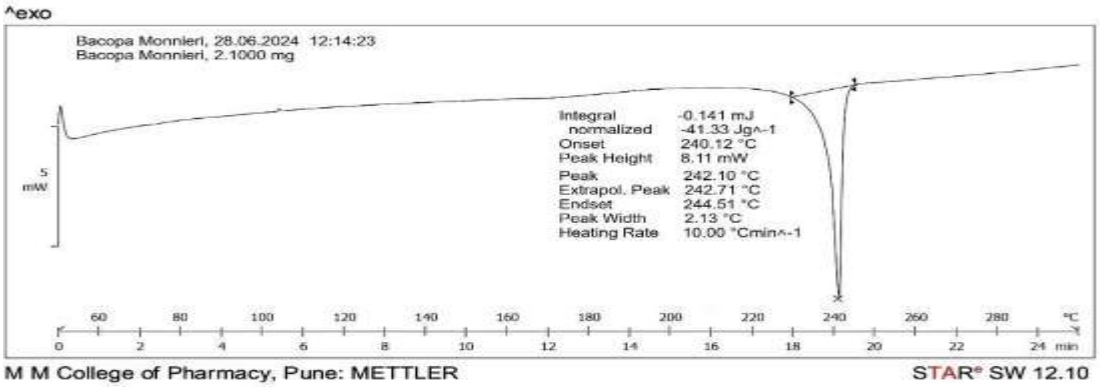

Figure 6: DSC of Bacoside A rich fraction

DSC thermogram of Bacoside A rich fraction + Bovine Colostrum can be observed in Fig. 7 below and it showed the peak at 242.25°C.

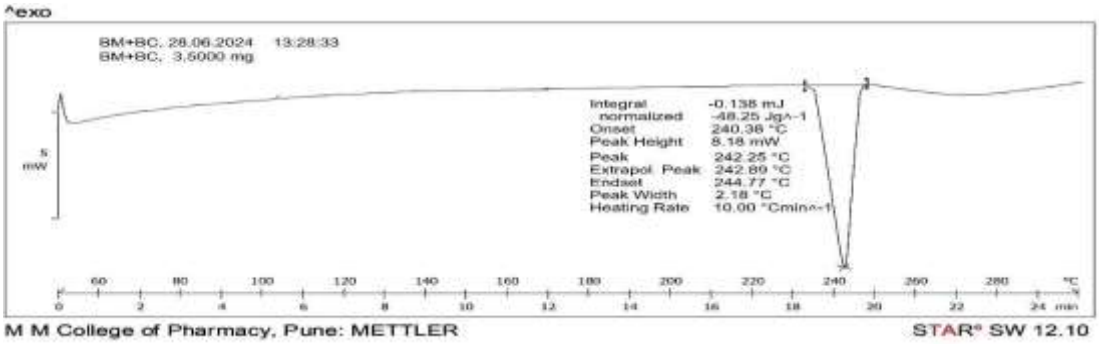

Figure 7: DSC of Bacoside A rich fraction + Bovine Colostrum

DSC thermogram of Physical mixture (Bacoside A rich fraction +Bovine colostrum: Span 60: Cholesterol) can be observed in Fig. 8 below and it showed the peak at 242.63°C.

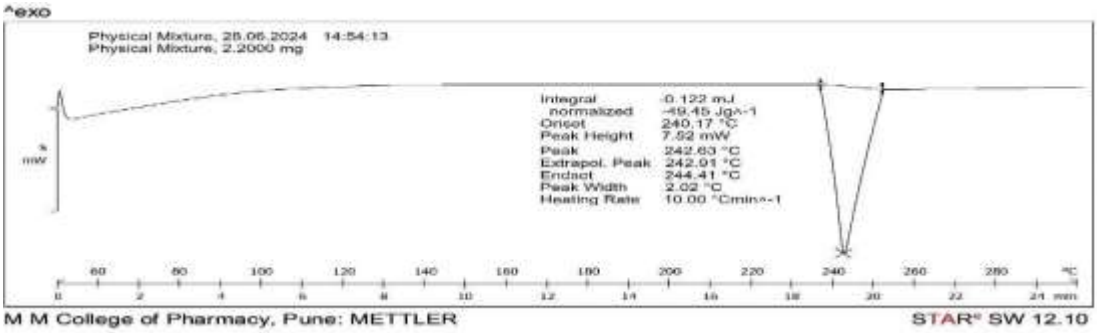

Figure 8: Physical mixture (Bacoside A rich fraction +Bovine colostrum: Span 60: Cholesterol)

3.1.7 X-ray Diffraction

The X-ray diffraction (XRD) pattern for the sample containing Bacoside A rich fraction +Bovine colostrum shows distinct peaks at 2 theta values: 10.12°, 15.19°, 17.12°, 17.95°, 18.35°, 19.45°, 22.12°, 24.19°, 25.14°, 25.45°, and 27.12°. These peaks indicate crystalline properties in the sample, with each peak corresponding to specific crystallographic planes. The high intensity peaks, particularly around 22.12° and 27.12°, suggest prominent crystallographic planes or higher crystallinity in those regions, while the lower intensity peaks reflect less ordered structures or smaller crystalline domains (Fig. 9). This data implies a structural interaction between the Bacoside A rich fraction and bovine colostrum. Further analysis, such as peak indexing or comparison with standard diffraction patterns, would provide more detailed insights into the molecular structure.

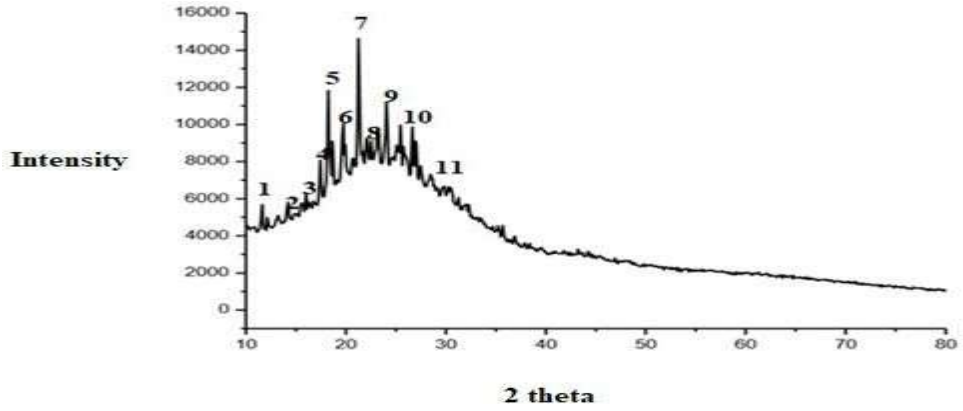

Figure 9: X-ray Diffraction of Bacoside A rich fraction +Bovine colostrum

The X-ray diffraction (XRD) pattern for the physical mixture of Bacoside A rich fraction + Bovine colostrum: Span 60: cholesterol shows distinct peaks at 2 theta values: 14.12°, 18.70°, 19.12°, 21.35°, 24.12°, 25.13°, and 28.19°. These peaks indicate the crystalline nature of the physical mixture. The prominent peaks, especially around 24.12° and 28.19°, suggest strong crystallographic planes, indicating higher crystallinity in those regions (Fig.10). This data suggests that the combination of Bacoside A fraction, bovine colostrum, Span 60, and cholesterol forms a stable crystalline structure, with key interactions between these components. Further analysis could explore the impact of these interactions on the material's properties, such as stability, solubility, or bioavailability. Comparing this pattern with individual components could also shed light on how the physical mixture alters the crystalline structure.

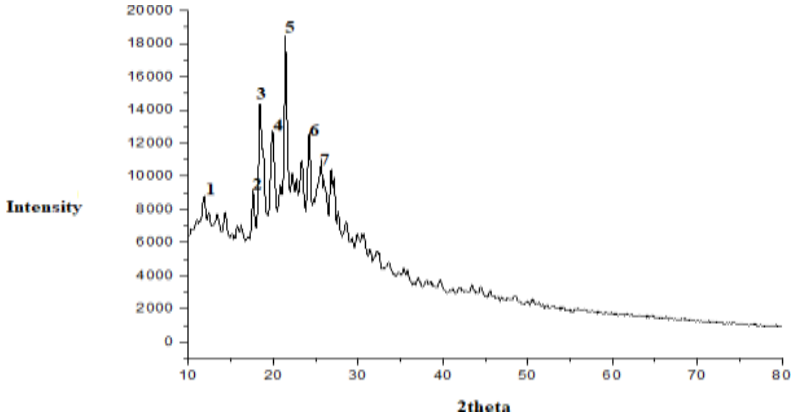

Figure 10: X-ray Diffraction of physical mixture (Bacoside A rich fraction + Bovine colostrum: Span 60: cholesterol)

3.2 POST FORMULATION STUDY

3.2.1 Particle Size and Polydispersity Index (PDI) analysis-

The analysis of particle size and polydispersity index (PDI) for Fort-BAF loadedniosomal formulations (BN1 to BN13) provides crucial insights into their potential as drug delivery

systems, with BN9 identified as the optimized formulation. It has been reported that particles smaller than 200nm could improve the bioavailability, stability and biological properties of drugs such as their pharmacokinetics and biodistribution. [54]

BN9 exhibits the smallest particle size at 121.7 ± 3.22 nm (Fig. 11), which is advantageous for enhancing bioavailability and enabling targeted delivery through improved membrane permeability and also confirming the capability of nanoparticles for oral drug delivery. As typical, bioavailability improved with a decrease in particle size [55]. Additionally, BN9 features a PDI of 0.06 ± 0.02, indicating a relatively narrow size distribution, which is essential for consistent drug release profiles. In contrast, other formulations, such as BN4, present larger sizes (265 ± 2.49 nm) and broader PDIs, which may impact their efficacy (Table 7). Overall, BN9 stands out as a strong candidate for further investigation due to its favorable particle size and low PDI. These findings underscore the importance of optimizing formulation parameters to achieve desired characteristics for effective therapeutic applications, with future studies focusing on the relationship between these physical properties and the performance of BN9 in drug release and bioactivity.

Table 7: Particle Size and Polydispersity Index of Fort-BAF loaded niosomes

Formulations	Particle Size	Polydispersity Index (PDI)
BN1	155± 2.44	0.02±0.01
BN2	162± 3.26	0.05±0.02
BN3	173± 2.86	0.03±0.01
BN4	265± 2.49	0.033±0.015
BN5	202± 2.86	0.025±0.002
BN6	179± 4.10	0.09±0.02
BN7	218± 4.49	0.021±0.010
BN8	127± 3.68	0.07±0.02
BN9	121.7±3.22	0.06±0.02
BN10	214± 3.26	0.015±0.002
BN11	245± 2.86	0.03±0.02
BN12	188± 4.08	0.034±0.0025
BN13	256± 3.29	0.07±0.02

All values expressed as Mean± S.D

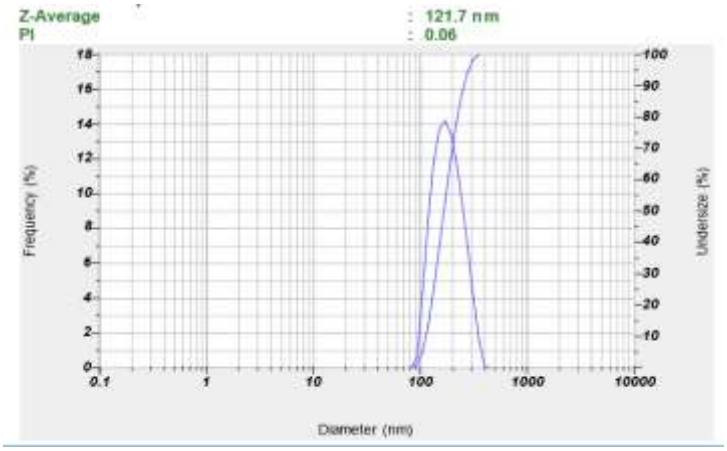

Figure 11: Particle size of Fort-BAF loaded niosomes Optimized batch (BN9)

ANOVA for Quadratic model

Response 3: Particle size

Source	Sum of Squares	df	Mean Square	F-value	p-value	
Model	24950.18	9	2772.24	16.03	0.0216	Significant
A-Span 60	1931.31	1	1931.31	11.17	0.0443	
B-Cholesterol	3362.00	1	3362.00	19.45	0.0216	
C-Hydration volume	766.36	1	766.36	4.43	0.1259	
AB	36.00	1	36.00	0.2082	0.6792	
AC	12802.92	1	12802.92	74.05	0.0033	
BC	324.00	1	324.00	1.87	0.2645	
A^2	1796.80	1	1796.80	10.39	0.0484	
B^2	1367.80	1	1367.80	7.91	0.0671	
C^2	737.49	1	737.49	4.27	0.1308	
Residual	518.67	3	172.89			
Cor Total	25468.85	12				

Factor coding is Coded.

Sum of squares is Type III - Partial

The Model F-value of 16.03 implies the model is significant. There is only a 2.16% chance that an F-value this large could occur due to noise.

P-values less than 0.0500 indicate model terms are significant. In this case A, B, AC, A^2 are significant model terms. Values greater than 0.1000 indicate the model terms are not significant. If there are many insignificant model terms (not counting those required to support hierarchy), model reduction may improve your model.

Fit Statistics

Std.Dev.	13.15	R^2	0.9796
Mean	192.75	Adjusted R^2	0.9185
C.V.%	6.82	PredictedR^2	0.9045
		Adeq Precision	12.5062

Final Equation in Terms of Coded Factors

Particle size=+214.00+15.54* A-20.50*B-9.79*C-3.00* AB+56.57* AC+9.00 *BC-28.04 *A^2-24.46* B^2+17.96*C

Final Equation in Terms of Actual Factors

Particle size=+623.09444+0.601250 *Span 60+0.891111*Cholesterol-119.71500*Hydration volume-0.003333*Span 60 * Cholesterol+0.754333*Span 60 * Hydration volume+0.120000*Cholesterol * Hydration volume-0.031153*Span 60^2-0.027181*Cholesterol^2+2.87400*Hydration volume^2

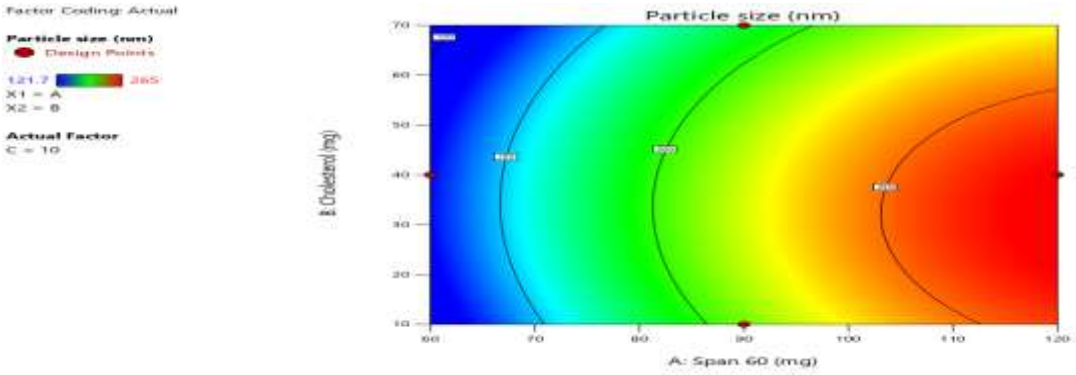

Figure 12: Counter plot of particle size of Niosomes

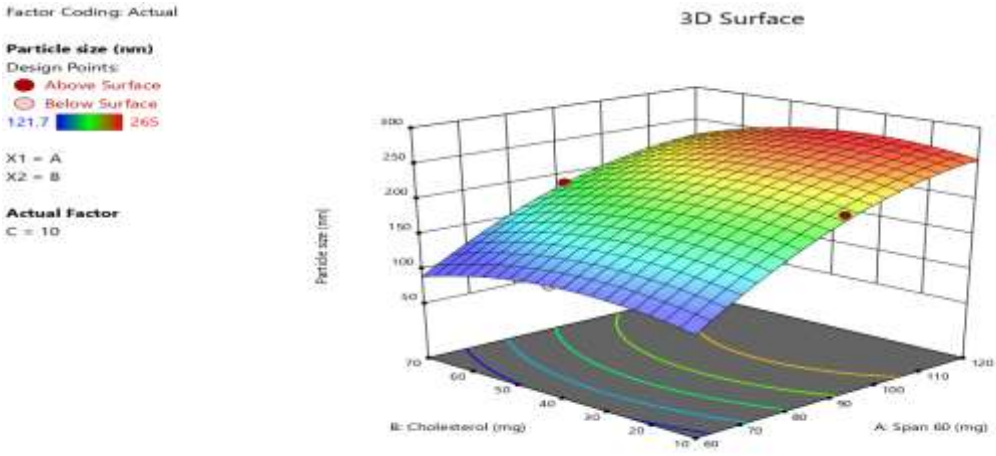

Figure 13: 3D surface plot of particle size of Niosomes

3.2.2 Zeta potentials

The zeta potential study of Fort-BAF loaded niosomal formulations (BN1–BN13) revealed a range of values from -9.26 mV to -28.5 mV, indicating varying colloidal stability across the formulations. Formulation BN9 exhibited the most negative zeta potential (-28.5 mV) (Fig. 14), suggesting it has the highest stability due to strong electrostatic repulsion, which minimizes particle aggregation. In contrast, BN6 had the least negative zeta potential (-9.26 mV), indicating lower stability and a higher risk of aggregation. Other formulations, such as BN3, BN5, BN8, andBN10, showed moderately high negative zeta potentials (above -25 mV), implying good stability. Overall, formulations with more negative zeta potentials, particularly BN9 and BN3, are likely to offer better physical stability and are more suitable for further development, while formulations with less negative values, like BN6 and BN12, may require optimization to enhance their stability.

Table 8:Zeta Potential of niosomes of (BN1-BN13)

Formulations	Zeta Potential (mV)
BN1	-21±0.123

BN2	-15.56±0.05
BN3	-27.23±0.06
BN4	-15.12±0.32
BN5	-25.56±0.03
BN6	-9.26±0.12
BN7	-19.23±0.541
BN8	-25.14±0.361
BN9	-28.5±0.02
BN10	-26.89±0.345
BN11	-13.48±0.987
BN12	-11.3±0.665
BN13	-14.12±0.354

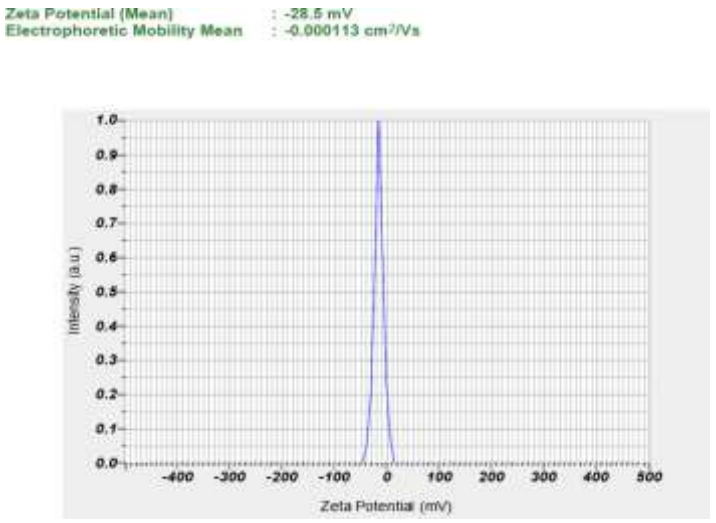

Figure 14: Zeta potential and PDI of Fort-BAF loaded optimized batch of niosomes (BN9)

ANOVA for Quadratic model

Response 2: Zeta potential

Source	Sum of Squares	df	Mean Square	F-value	p-value	
Model	534.20	9	59.36	14.96	0.0238	Significant
A-Span 60	7.45	1	7.45	1.88	0.2641	
B-Cholesterol	40.55	1	40.55	10.22	0.0495	
C-Hydration volume	9.01	1	9.01	2.27	0.2289	
AB	49.98	1	49.98	12.60	0.0381	
AC	181.17	1	181.17	45.67	0.0066	
BC	3.44	1	3.44	0.8674	0.4204	
A^2	5.00	1	5.00	1.26	0.3434	
B^2	98.18	1	98.18	24.75	0.0156	
C^2	112.60	1	112.60	28.38	0.0129	
Residual	11.90	3	3.97			
CorTotal	546.10	12				

Factor coding is Coded.

Sum of squares is Type III - Partial

The Model F-value of 14.96 implies the model is significant. There is only a 2.38% chance that an F-value this large could occur due to noise.

P-values less than 0.0500 indicate model terms are significant. In this case B, AB, AC, B^2, C^2 are significant model terms. Values greater than 0.1000 indicate the model terms are not significant. If there are many insignificant model terms (not counting those required to support hierarchy), model reduction may improve your model.

Fit Statistics

Std.Dev.	1.99	R^2	0.9782
Mean	-19.45	Adjusted R^2	0.9128
C.V.%	10.24	PredictedR^2	0.9046
		Adeq Precision	10.9757

Final Equation in Terms of Coded Factors

Zeta potential=-26.89+0.9650* A+2.25* B-1.06* C+3.53* AB+6.73* AC+0.9275* BC-1.48* A^2+6.55* B+7.02* C^2

Final Equation in Terms of Actual Factors

Zeta potential =+110.32819-0.502194*Span 60-0.953764*Cholesterol-25.84017*Hydration volume+0.003928*Span 60 * Cholesterol+0.089733*Span 60 * Hydration volume+0.012367*Cholesterol * Hydration volume-0.001643*Span 60^2+0.007282*$Cholesterol^2$+1.12300*$Hydration\ volume^2$

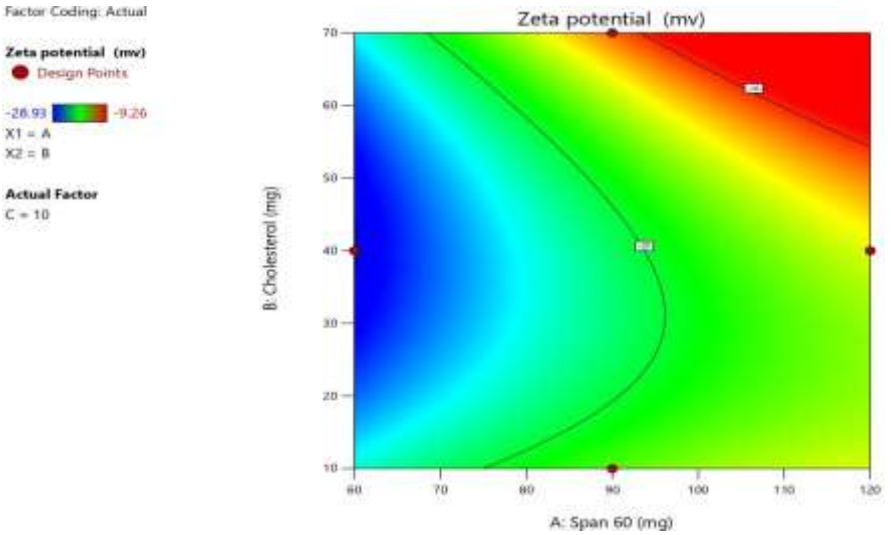

Figure15:Counter plot of zeta potential of Niosomes

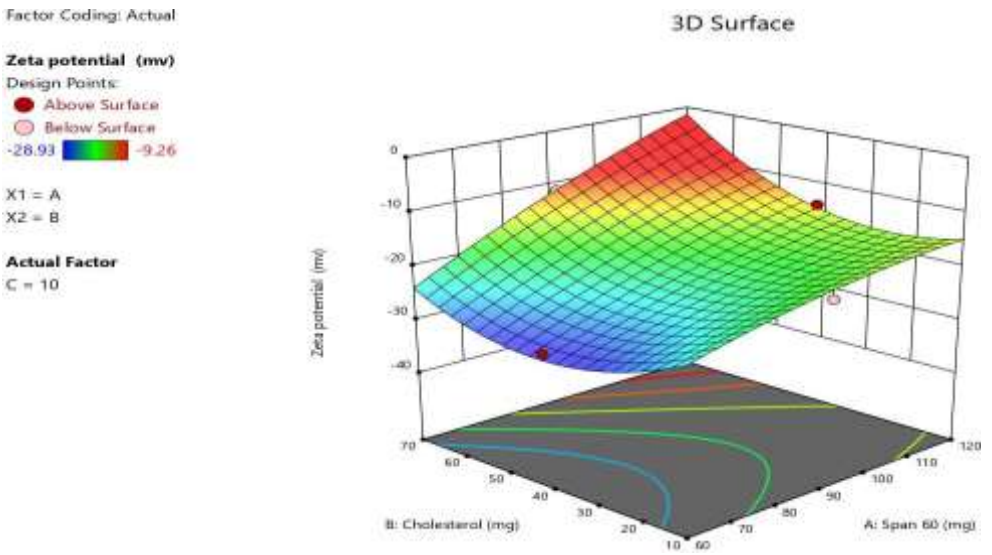

Figure16:3D Surface plot of zeta potential of Niosomes

3.2.3 Entrapment efficiency

The entrapment efficiency of the niosomes was assessed across formulations BN1 to BN13, revealing a range of efficiencies. Among these, formulation BN9 exhibited the highest entrapment efficiency at 87.56%, significantly outperforming the other formulations. This indicates that BN9 is particularly effective in encapsulating the active compound, making it the most promising candidate for drug delivery applications. In contrast, the lowest entrapment efficiency was recorded in BN4 at 52.36% (Table 9). Overall, these results underscore the potential of niosomal formulations, particularly BN9, in enhancing the delivery and stability of the therapeutic agents.

Table 9: Entrapment Efficiency (%) of niosomes (BN1-BN13)

Formulations	Entrapment Efficiency (%)
BN1	58
BN2	54
BN3	68.12
BN4	52.36
BN5	54.69
BN6	60
BN7	65.9
BN8	78
BN9	87.56
BN10	62.36
BN11	58.25
BN12	70.56
BN13	65.56

ANOVA for 2FI model

Response 1: Entrapment efficiency (%)

Source	Sum of Squares	df	Mean Square	F-value	p-value	
Model	1012.20	6	168.70	4.73	0.0402	Significant
A-Span 60	140.70	1	140.70	3.95	0.0942	
B-Cholesterol	82.69	1	82.69	2.32	0.1787	
C-Hydration volume	323.22	1	323.22	9.06	0.0237	
AB	107.02	1	107.02	3.00	0.1339	
AC	356.45	1	356.45	10.00	0.0195	
BC	2.12	1	2.12	0.0594	0.8156	
Residual	213.98	6	35.66			
CorTotal	1226.17	12				

Factor coding is Coded.

Sum of squares is Type III - Partial

The Model F-value of 4.73 implies the model is significant. There is only a 4.02% chance that an F-value this large could occur due to noise.

P-values less than 0.0500 indicate model terms are significant. In this case C, AC are significant model terms. Values greater than 0.1000 indicate the model terms are not significant. If there are many insignificant model terms (not counting those required to support hierarchy), model reduction may improve your model.

Fit Statistics

Std. Dev.	5.97	R^2	0.8255
Mean	64.26	Adjusted R^2	0.6510
C.V.%	9.29	PredictedR^2	0.0380
		Adeq Precision	7.2094

The Predicted R^2 of 0.0380 is not as close to the Adjusted R^2 of 0.6510 as one might normally expect; i.e. the difference is more than 0.2. This may indicate a large block effect or a possible problem with your model and/or data. Things to consider are model reduction, response transformation, outliers, etc. All empirical models should be tested by doing confirmation runs.

Adeq Precision measures the signal to noise ratio. A ratio greater than 4 is desirable. Your ratio of 7.209 indicates an adequate signal. This model can be used to navigate the design space.

Final Equation in Terms of Coded Factors

Entrapment efficiency (%) = +64.26-4.19* A+3.21 *B+6.36* C-5.17* AB9.44*AC +0.7275*BC

Final Equation in Terms of Actual Factors

Entrapment efficiency (%) = -49.25571+1.03410*Span 60+0.551667*Cholesterol + 13.48250*Hydration volume - 0.005747Span 60 * Cholesterol0.125867Span 60 * Hydration volume + 0.009700 Cholesterol * Hydration volume

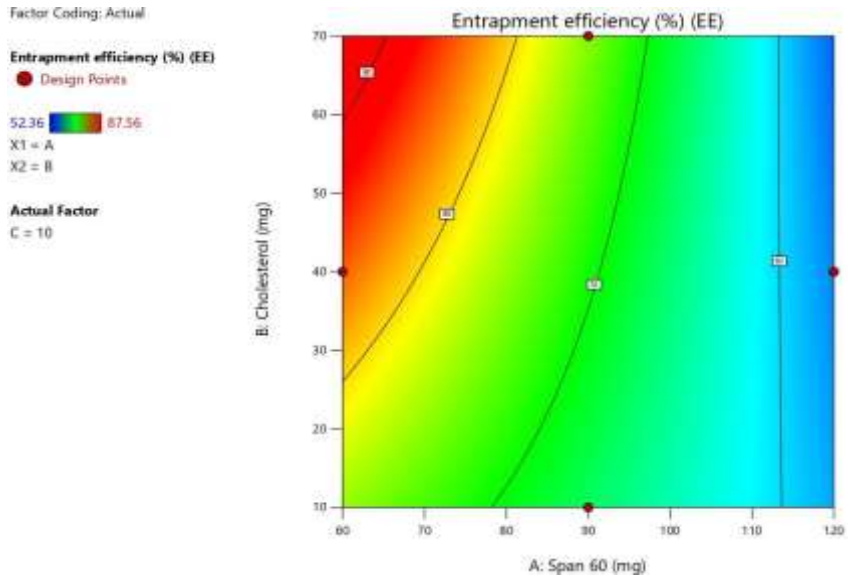

Figure17: Counter plot of Entrapment efficiency(EE%)of Niosome

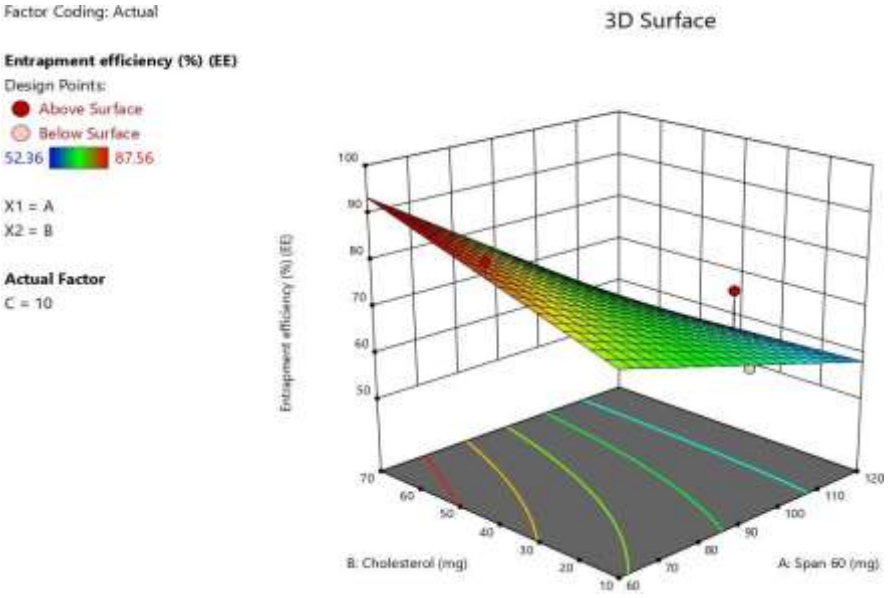

Figure18: 3D Surface plot of Entrapment efficiency (EE%) of noisome

3.2.4 Fourier Transform Infra-Red-Spectroscopy (FTIR)

The FTIR spectrum of the Fort-BAF loaded niosome optimized batch (BN9) demonstrates significant functional groups indicative of successful encapsulation and stability of the active compounds. The O–H stretching observed at 3275.5 and 2932.23 cm^{-1} aligns closely with reported values, confirming the presence of hydroxyl groups essential for interaction and

solubility. The –C≡C– stretch at 2123.24 cm^{-1} suggests effective incorporation of alkynes, while the C=O stretches at 1626.66 and 1601.59 cm^{-1} indicate the presence of carbonyl groups, vital for the niosomes chemical structure. Additionally, the N–O asymmetric stretch at 1508.06 cm^{-1} and C–C stretch in-ring at 1427.07 cm^{-1} further corroborate the functional integrity of the bioactive components. The various C–H bending vibrations observed between 918.914 and 774.279 cm^{-1} are consistent with reported ranges, highlighting the niosomes complex molecular interactions. Furthermore, the presence of multiple C–N stretches ranging from 1024.02 to 1265.07 cm^{-1} reflects the involvement of nitrogen-containing groups, which may enhance the formulation's stability and functionality. Overall, these spectral characteristics validate the successful formulation of BN9, suggesting that the niosomal delivery system effectively retains the bioactive properties of Bacoside A for enhanced therapeutic applications. (Fig. 19)

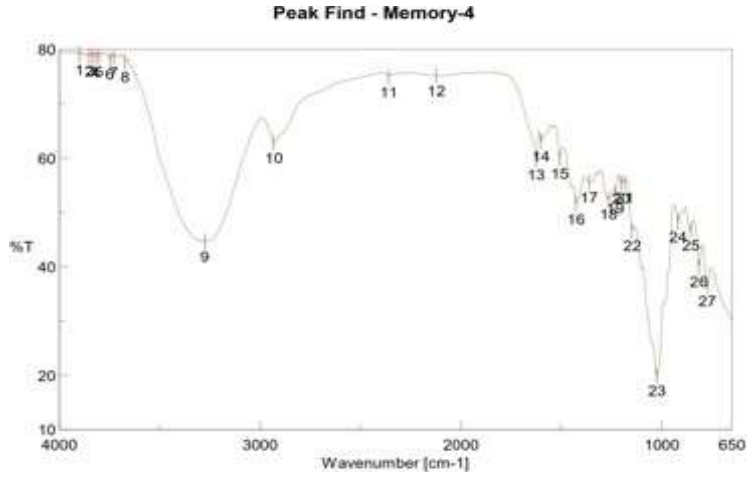

Figure19:FTIR Spectrum of Fort-BAF loaded noisome optimized batch(BN9)

3.2.5 Differential Scanning Calorimetry (DSC)

Optimized BN9 batch niosomal formulation shows a slight peak, corresponding probably to the melting point at 241.580C.

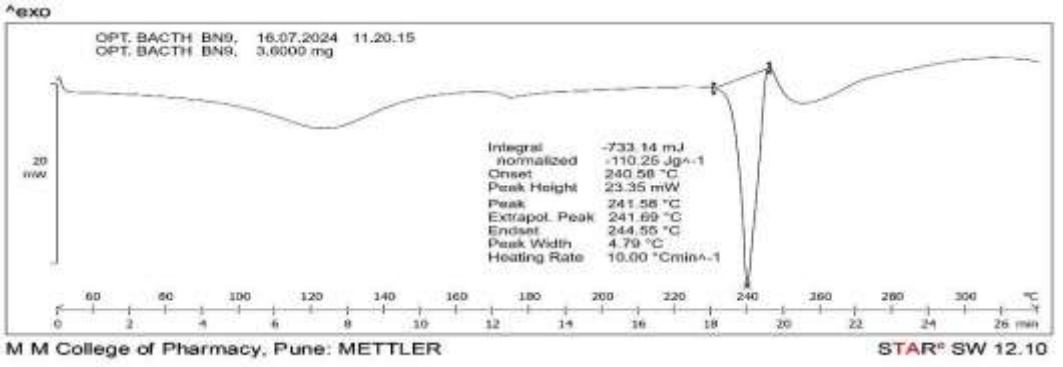

Figure20: Spectrum of DSC of Fort-BAF loaded noisome optimized batch(BN9)

3.2.6 X-ray Diffraction

The XRD Diffractogram of the Fort-BAF loaded niosome optimized batch (BN9) displays distinct peaks at 2 theta values of 5.95°, 9.25°, 12.45°, 13.95°, 15.25°, and 19.29°, indicating its crystalline nature (Fig. 21). These sharp peaks suggest a high degree of crystallinity, which is vital for the stability and consistent performance of the niosomal drug delivery system. This crystallinity may enhance the stability and bioavailability of the encapsulated Bacoside A, supporting the effectiveness of the BN9 formulation in therapeutic applications.

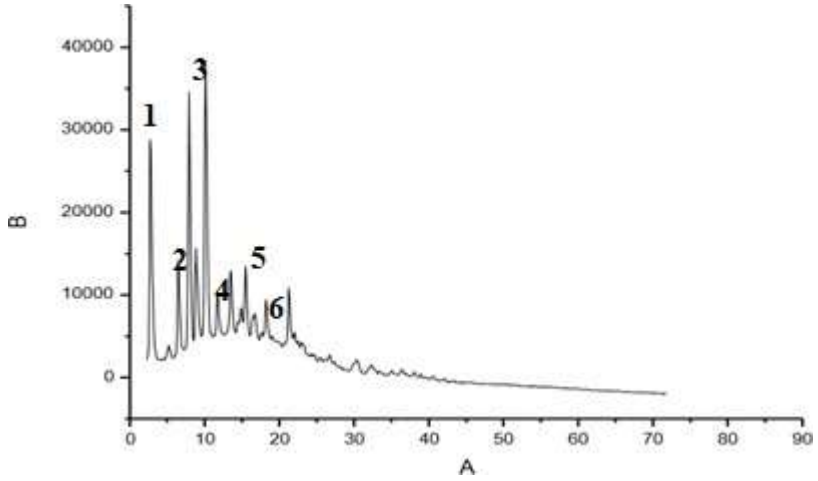

Figure21:XRD Diffractogram of Fort-BAF loaded noisome optimized batch (BN9)

3.2.7 Scanning Electron Microscopy (SEM)

The SEM micrograph of the optimized niosomal formulation (BN9) shows a range of particle sizes (4.9 nm to 19.48 nm), indicating effective encapsulation of Bacoside A fraction and Bovine colostrum. The well-defined structures suggest enhanced stability and bioavailability, supporting the formulation's high entrapment efficiency.

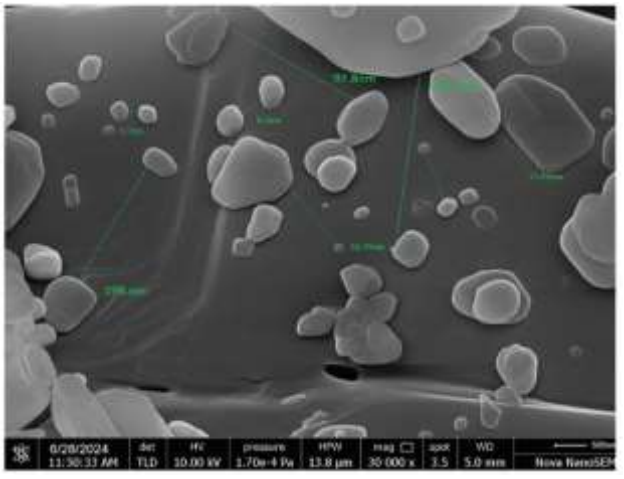

Figure22:Scanning electron microscopy (SEM) micrographs of optimized batch (BN9)

3.2.8 Transmission Electron Microscopy (TEM):

The TEM micrographs represent a comparative analysis between Fort-BAF loaded niosomes (A) and blank niosomes (B), both at a scale of 200 nm. In image A, representing the Fort-BAF loaded niosomes (BN9 optimized batch), the particles appear uniformly distributed with distinct spherical morphology, indicating a successful encapsulation and stable niosome formation. The size and shape consistency reflect good batch optimization with minimal aggregation. In contrast, image B displays the blank niosomes, which show a higher degree of size variation and irregularities in particle shape. The lack of uniformity in blank niosomes suggests potential instability or less controlled formation processes. This comparison highlights that the Fort-BAF loaded niosomes (A) exhibit more stable and homogeneous characteristics compared to the blank niosomes (B), confirming the successful optimization of the BN9 batch.

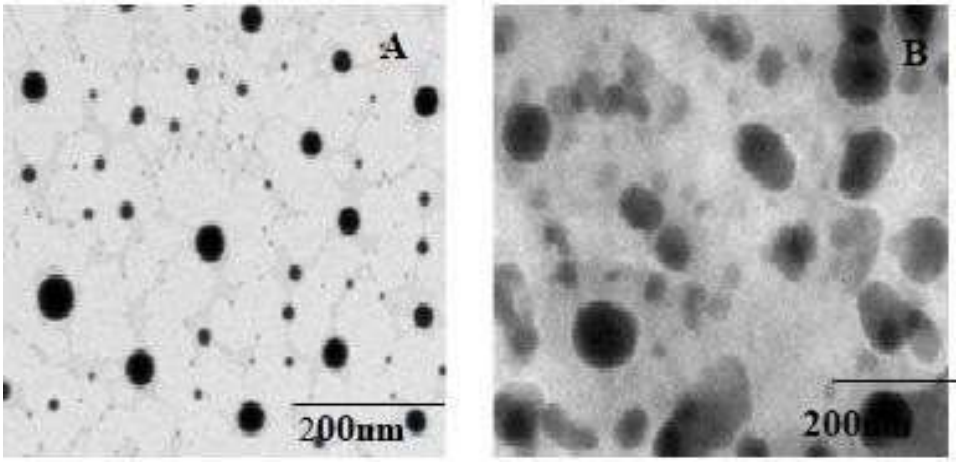

Figure23:Transmission electron microscopy (TEM) micrographs of A-Fort-BAF loaded niosomes optimized batch (BN9) at 200nm, B-Blank niosome

3.2.9. In-Vitro Drug Release Studies:

Table 10: In-vitro release study of drug

Formulation Code	TimeinMin. 0Time	10Time	15Time	30Time	45Time	60Time
BN1	0	34.17%	36.17%	43.83%	64.80%	73.32%
BN2	0	36.25%	38.39%	40.25%	47.06%	55.42%
BN3	0	32.83%	47.14%	63.45%	65.59%	69.74%
BN4	0	36.46%	43.57%	52.38%	58.28%	60.42%
BN5	0	45.46%	50.57%	55.26%	59.20%	61.42%
BN6	0	37.46%	39.57%	42.26%	59.28%	60.42%
BN7	0	30.17%	36.17%	43.83%	64.80%	69.32%
BN8	0	40.22%	42.30%	45.45%	50.36%	55.40%
BN9	0	41.17%	45.39%	55.65%	68.36%	75.42%
BN10	0	30.46%	35.57%	39.26%	42.28%	49.42%
BN11	0	33.46%	35.57%	39.26%	41.28%	42.42%
BN12	0	35.4%	39.45%	42.15%	59.05%	59.28%
BN13	0	37.89%	39.5%	42.26%	59.28%	61.36%

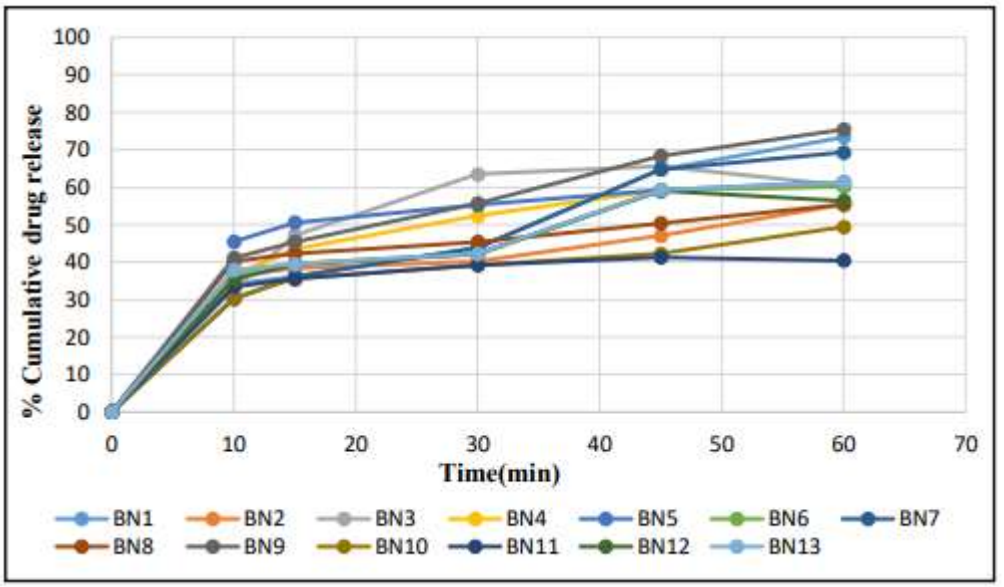

Figure 24:%Cumulativedrugrelease(BN1-BN13)

The in vitro release profile study was carried out using Franz diffusion cell concludes the amount of drug release from the fibers on the skin from niosomes on was found to be BN9 up to 1 hr. The in vitro release profile study conducted using a Franz diffusion cell conclusively determined that 75.42% of the drug from batch permeated through the skin and was released within 1 hour.

Kinetic analysis of drug release

In order to define the release mechanism that gives the best description of the release pattern; the in vitro release data for all optimized batches were fitted to kinetic equations models.The kinetic equations were used i.e., zero, first-order and Higuchi model. Both the kinetic rate constant (k) and the determination coefficient (R2) were calculated and presented in above graphs. The best fit model with the highest determination coefficient (R2) value for all optimized batches was Higuchi model. (Table 11)

Table 11: TimeVs%CumulativeKineticDrug Release

Formulation Code	RegressionCoefficient(R^2)		
	ZeroOrder	FirstOrder	HiguchiOrder
BN1	0.8937	0.5116	0.8937
BN2	0.6836	0.4254	0.6836
BN3	0.6614	0.4456	0.6614
BN4	0.7099	0.4385	0.7099
BN5	0.9288	0.3912	0.9288
BN6	0.7464	0.4493	0.7464
BN7	0.8956	0.5225	0.8956
BN8	0.6061	0.4014	0.6061
BN9	0.8096	0.4653	0.8096
BN10	0.6877	0.4319	0.6877
BN11	0.5316	0.3857	0.5316
BN12	0.7258	0.4462	0.7258
BN13	0.7551	0.4515	0.7551

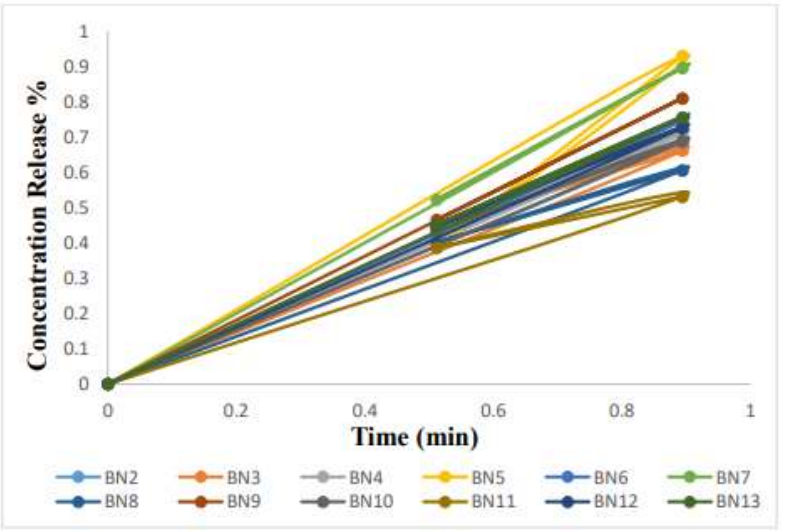

Figure 25: In vitro drug release profile Time vs. %cumulative drug release

3.2.10 Stability Study:

The stability study of the Fort-BAF loadedoptimized niosomes formulation (BN9) over a three-month period showed minimal changes in particle size, zeta potential, and entrapment efficiency, indicating excellent stability. The particle size remained almost constant, with only a slight decrease from 121.7 nm at "0" month to 121.5 nm at the third month. The zeta potential remained stable at - 28.5 mV throughout, with a negligible shift to -28.4 mV by the third month, indicating that the colloidal stability was preserved. The entrapment efficiency also exhibited minimal variation, from 87.56% initially to 87.53% after three months. Overall, the formulation demonstrated strong stability over the storage period, maintaining its key characteristics with minimal degradation or changes.(Table 12)

Table 12: Effect of storage on particle size, zeta potential and entrapment Efficiency of optimized niosomes formulation (BN9)

Storage time	"0" Month	"1" Month	"2" Month	"3" Month
Particle size (nm)	121.7±0.123	121.7±0.122	121.5±0.124	121.5±0.121
Zeta potential (mV)	-28.5±0.05	-28.5±0.05	-28.5±0.04	-28.4±0.03
Entrapment Efficiency (%)	87.56±0.05	87.56±0.05	87.56±0.04	87.53±0.03

Values are expressed as mean ±SD

3.3. IN VIVO STUDY

3.3.1. Morris water test model

Learning and memory are linked with Escape Latency (EP) and time spent in target quadrant (TSTQ). Decline of EP and augment of TSTQ by mice in Morris water maze reflect enhancement of memory and learning. The Fort-BAF loadedoptimized Niosomal formulation (BN9)were fed for 18 consecutive days, significantly lowered EP of mice from

14th to 17th day and augmentation of TSTQ by mice on 18th day as compared to the control and demonstrated priceless enhancement of learning and memory. The results observed are given below. (Table 13 and 14)

Table 13: Effect of Bacoside A rich fraction and Optimised Niosomal formulation (BN9) on escape latency in Morris water test model.

Treatment Schedule	Escape Latency (EP) 14^{th}	Escape Latency (EP) 15^{th}	Escape Latency (EP) 16^{th}	Escape Latency (EP) 17^{th}
Control	23.45±0.91 ^{ns}	21.17±0.35 ^{ns}	22.85±2.09 ^{ns}	19.67±0.36 ^{ns}
CMC	90.11±1.38*	92.48±0.59*	91.48±1.05*	93.78±1.06*
Piracetam injection i.p.	29.47±0.92**	32.78±0.57**	30.56±0.58**	31.44±0.98**
Bacoside A rich fraction (200mg/kg)	56.02±1.97**	54.89±1.64**	52.01±2.09**	55.37±1.25**
Optimised Niosomal formulation (BN9)(200mg/kg)	40.02±0.97**	42.89±0.94**	39.01±0.79**	38.17±0.75**

The results are expressed as mean ± SD (n = 6) escape latency time in second. Ns is non-significant where, $p>0.05$, $^{**}p<0.001$ and $^{*}p<0.01$ indicates very significant, and significant levels of significance.

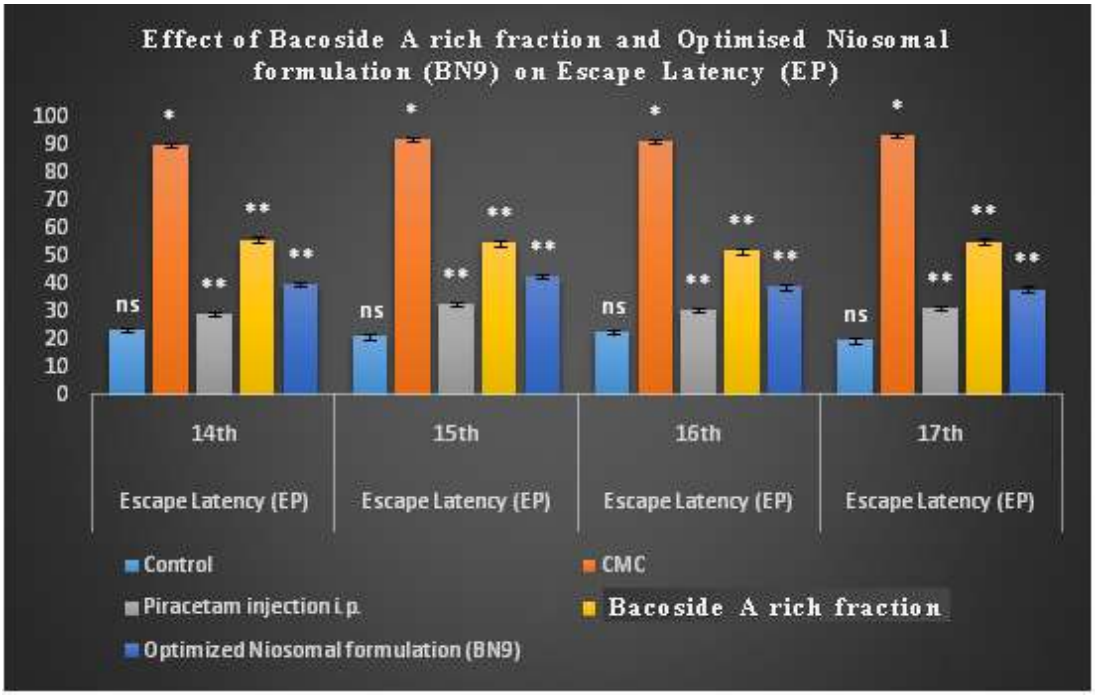

Figure 26: Effect of Bacoside A rich fraction and Optimised Niosomal formulation (BN9) on Escape Latency (EP)

Table 14: Effect of Bacoside A rich fraction and Optimised Niosomal formulation (BN9) on time spent in target quadrant (TSTQ).

Treatment Schedule	Time spent (sec) in target quadrant (18th day)
Control	63.76±0.79
CMC	23.68±1.39$^{@}$
Piracetam injection i.p.	54.96±2.01**

Bacoside A rich fraction (200mg/kg)	40.78±1.89**
Optimized Niosomal formulation (BN9) (200mg/kg)	33.56±0.98**

All values are in second

The results were expressed as mean SD (n = 6), **p<0.01, very significant; when compared to CMC group. @ p<0.01, when compared with control group

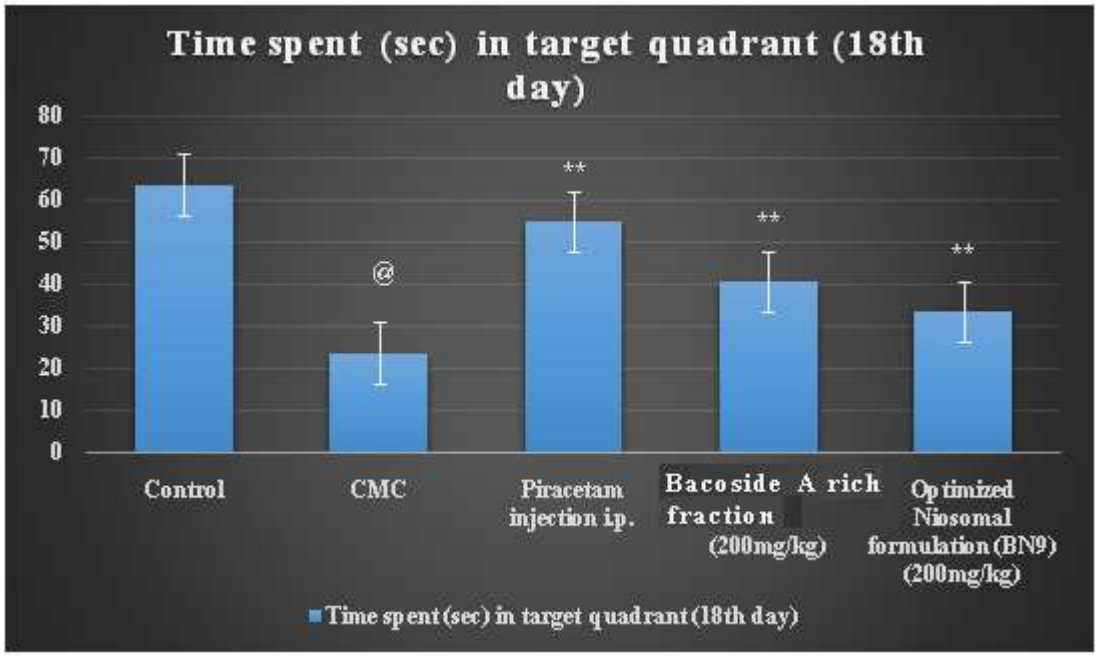

Figure 27: Effect of Bacoside A rich fraction and Optimised Niosomal formulation (BN9) on time spent in target quadrant (TSTQ).

3.3.2. Y- Maze Task

On oral administration, Optimized Niosomal formulation (BN9), correspondingly produced important (P < 0.01) amplify in the percentage of number of open arm entries and time spent in open arm but in closed arm, number of entries and time spent was extensively (P < 0.01) decreased when compared with vehicle-treated group.(Table 15)

Table 15: Effect of Bacoside A rich fraction and Optimised Niosomal formulation (BN9) on open and closed entries.

Treatment Schedule	No of Entries %		Time Spent (Sec)	
	Open Arm	Closed Arm	Open Arm	Closed Arm
Control	57.62±0.94	43.21±1.07	102.34±1.56	78.64±1.24
CMC	27.08±0.79@	72.92±1.06@	68.32±1.25@	111.61±1.03@
Piracetam injection i.p.	30.54±1.77**	69.46±1.76**	59.35±1.65**	120.67±1.44**
Bacoside A rich fraction(200mg/kg)	42.54±0.87**	57.46±1.26**	77.35±1.05**	102.67±2.04**
Optimized Niosomal formulation (BN9)	33.25±0.86**	66.75±0.86**	84.21±1.78**	95.39±0.97**

The results were expressed as mean SD (n = 6), **p<0.01, very significant; when compared to CMC group. @ p<0.01, when compared with control group.

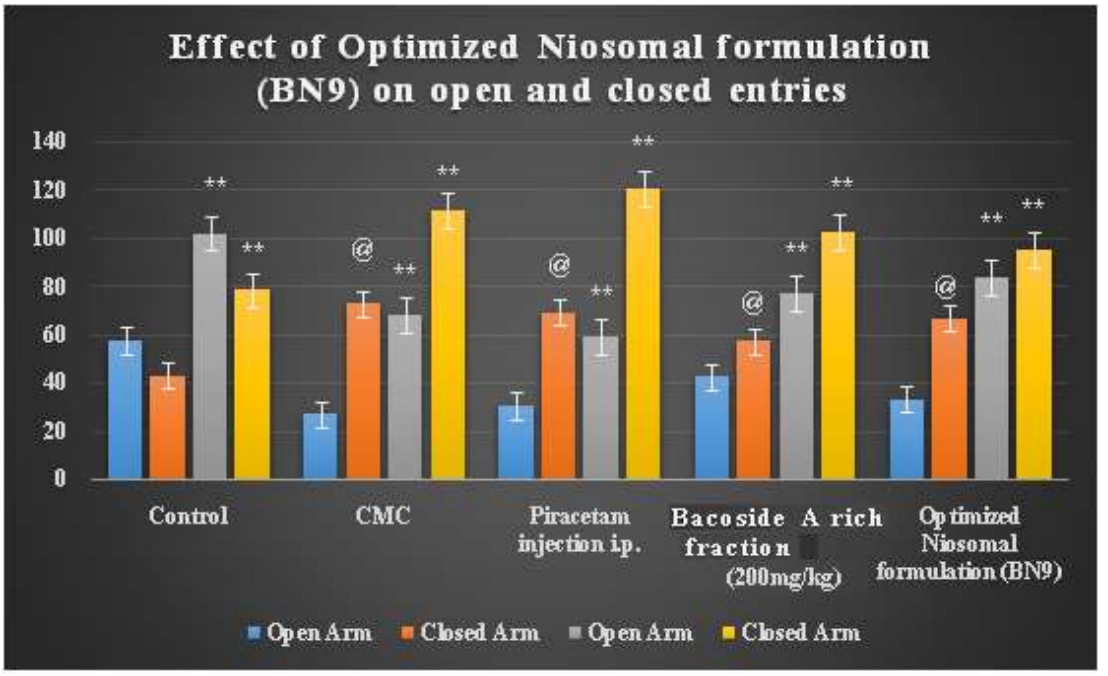

Figure 28: Effect of Bacoside A rich fraction and Optimised Niosomal formulation (BN9) on an open and closed entries

4. CONCLUSION

An inventive and successful method of drug delivery is shown by the development and evaluation of niosomes that contain bovine colostrum and bacoside A. To optimise the noisome formulations using desirability criteria, Box Behnken design was employed. With its small particle size, high entrapment efficiency, and outstanding zeta potential, the optimised formulation BN9 demonstrated exceptional qualities that suggested it could have improved stability and bioavailability. Both the structural integrity and compatibility of the niosomal system were validated by the thorough evaluation conducted through pre- and post-formulation studies. According to the results of an in-vivo study, BN 9 was effective at improving learning and memory and reversed the cognitive deficits that scopolamine had caused in mice. This suggests that BN 9 may be useful in conditions related to memory dysfunctions. With increased drug stability and bioavailability, the results show that Fort-BAF loaded niosomes have a promising role in developing therapeutic approaches for neuroprotection and cognitive enhancement, opening the door for more study and clinical applications in this field. Nowadays, the focus is on enhancing people's quality of life overall as well as developing novel treatments for human illness.

CONFLICT OF INTEREST

All authors declare that there is no any conflict of interest.

References

1. Khare, C. P. (Ed.). (2011). Indian herbal remedies: rational western therapy, ayurvedic and other traditional usage, botany. Springer science & business media.
2. Singh, H. K., & Dhawan, B. N. (1982). Effect of Bacopa monniera Linn.(Brāhmi) extract on avoidance responses in rat. Journal of ethnopharmacology, 5(2), 205-214.
3. Chaudhari, K. S., Tiwari, N. R., Tiwari, R. R., & Sharma, R. S. (2017). Neurocognitive effect of nootropic drug Brahmi (Bacopa monnieri) in Alzheimer's disease. Annals of neurosciences, 24(2), 111-122.
4. Murthy, H. N. (2022). Biotechnological production of bacosides from cell and organ cultures of Bacopa monnieri. Applied microbiology and biotechnology, 106(5), 1799-1811.
5. Mateev, E., Kondeva-Burdina, M., Georgieva, M., & Zlatkov, A. (2023). Repurposing of FDA-approved drugs as dual-acting MAO-B and AChE inhibitors against Alzheimer's disease: An in silico and in vitro study. Journal of Molecular Graphics and Modelling, 122, 108471.
6. Srivastava, S., Ahmad, R., & Khare, S. K. (2021). Alzheimer's disease and its treatment by different approaches: A review. European Journal of Medicinal Chemistry, 216, 113320.
7. Bhatia, S., Singh, M., Sharma, P., Mujwar, S., Singh, V., Mishra, K. K., & Ahmad, S. F. (2023). Scaffold Morphing and In Silico Design of Potential BACE-1 (β-Secretase) Inhibitors: A Hope for a Newer Dawn in Anti-Alzheimer Therapeutics. Molecules, 28(16), 6032.
8. Rajan, K. E., Preethi, J., & Singh, H. K. (2015). Molecular and functional characterization of Bacopa monniera: a retrospective review. Evidence-Based Complementary and Alternative Medicine, 2015(1), 945217.
9. Abdul Manap, A. S., Vijayabalan, S., Madhavan, P., Chia, Y. Y., Arya, A., Wong, E. H., & Koshy, S. (2019). Bacopa monnieri , a neuroprotective lead in Alzheimer disease: a review on its properties, mechanisms of action, and preclinical and clinical studies. Drug target insights, 13, 1177392819866412.
10. Chakravarty, A. K., Sarkar, T., Masuda, K., Shiojima, K., Nakane, T., & Kawahara, N. (2001). Bacopaside I and II: two pseudojujubogenin glycosides from Bacopa monniera. Phytochemistry, 58(4), 553-556.
11. Rastogi, S., Pal, R., & Kulshreshtha, D. K. (1994). Bacoside A3□ A triterpenoid saponin from Bacopa monniera. Phytochemistry, 36(1), 133-137.
12. Sivaramakrishna, C., Rao, C. V., Trimurtulu, G., Vanisree, M., &Subbaraju, G. V. (2005). Triterpenoid glycosides from Bacopa monnieri . Phytochemistry, 66(23), 2719-2728.
13. Garai, S., Mahato, S. B., Ohtani, K., & Yamasaki, K. (1996). Dammarane-type triterpenoid saponins from Bacopa monniera. Phytochemistry, 42(3), 815-820.
14. Saraf, M. K., Prabhakar, S., Khanduja, K. L., & Anand, A. (2011). Bacopa monniera attenuates scopolamine-induced impairment of spatial memory in mice. Evidence-Based Complementary and Alternative Medicine, 2011(1), 236186.
15. Mukherjee, S., Dugad, S., Bhandare, R., Pawar, N., Jagtap, S., Pawar, P. K., & Kulkarni, O. (2011). Evaluation of comparative free-radical quenching potential of Brahmi (Bacopa monnieri) and Mandookparni (Centella asiatica). AYU (An International Quarterly Journal of Research in Ayurveda), 32(2), 258-264.
16. Malishev, R., Shaham-Niv, S., Nandi, S., Kolusheva, S., Gazit, E., & Jelinek, R. (2017). Bacoside-A, an Indian traditional-medicine substance, inhibits β-amyloid cytotoxicity, fibrillation, and membrane interactions. ACS chemical neuroscience, 8(4), 884-891.
17. Holcomb, L. A., Dhanasekaran, M., Hitt, A. R., Young, K. A., Riggs, M., & Manyam, B. V. (2006). Bacopa monniera extract reduces amyloid levels in PSAPP mice. Journal of Alzheimer's Disease, 9(3), 243-251.
18. Limpeanchob, N., Jaipan, S., Rattanakaruna, S., Phrompittayarat, W., &Ingkaninan, K. (2008). Neuroprotective effect of Bacopa monnieri on beta-amyloid-induced cell death in primary cortical culture. Journal of ethnopharmacology, 120(1), 112-117.

19. Sekhar, V. C., Viswanathan, G., & Baby, S. (2019). Insights into the molecular aspects of neuroprotective bacoside A and bacopaside I. Current neuropharmacology, 17(5), 438-446.
20. Kim, S. E., Ko, I. G., Shin, M. S., Kim, C. J., Ko, Y. G., & Cho, H. (2012). Neuroprotective effects of bovine colostrum on intracerebral hemorrhage-induced apoptotic neuronal cell death in rats☆. Neural Regeneration Research, 7(22), 1715-1721.
21. Schuster, D., Rajendran, A., Hui, S. W., Nicotera, T., Srikrishnan, T., & Kruzel, M. L. (2005). Protective effect of colostrinin on neuroblastoma cell survival is due to reduced aggregation of β-amyloid. Neuropeptides, 39(4), 419-426.
22. Sochocka, M., Ochnik, M., Sobczyński, M., Siemieniec, I., Orzechowska, B., Naporowski, P., & Leszek, J. (2019). New therapeutic targeting of Alzheimer's disease with the potential use of proline-rich polypeptide complex to modulate an innate immune response-preliminary study. Journal of Neuroinflammation, 16, 1-16.
23. Popik, P., Galoch, Z., Janusz, M., Lisowski, J., &Vetulani, J. (2001). Cognitive effects of Colostral-Val nonapeptide in aged rats. Behavioural brain research, 118(2), 201-208.
24. Bilikiewicz, A., &Gaus, W. (2004). Colostrinin (a naturally occurring, proline-rich, polypeptide mixture) in the treatment of Alzheimer's disease. Journal of Alzheimer's Disease, 6(1), 17-26.
25. Superti, F. (2020). Lactoferrin from bovine milk: a protective companion for life. Nutrients, 12(9), 2562.
26. Subramanian, P. (2021). Lipid-based nanocarrier system for the effective delivery of nutraceuticals. Molecules, 26(18), 5510.
27. Moammeri, A., Chegeni, M. M., Sahrayi, H., Ghafelehbashi, R., Memarzadeh, F., Mansouri, A., & Ren, Q. (2023). Current advances in niosomes applications for drug delivery and cancer treatment. Materials Today Bio, 23, 100837.
28. Jose, S., Sowmya, S., Cinu, T. A., Aleykutty, N. A., Thomas, S., & Souto, E. B. (2014). Surface modified PLGA nanoparticles for brain targeting of Bacoside-A. European Journal of Pharmaceutical Sciences, 63, 29-35.
29. Vitthal, K. U., Pillai, M. M., &Kininge, P. (2013). Study of solid lipid nanoparticles as a carrier for bacoside. Int. J. Pharma Biosci, 3, 414-426.
30. Kumar, R., & Garg, R. (2020). Formulation and evaluation of solid lipid nanoparticles loaded with bacoside rich extract. Int J Pharm Sci Res, 11(1), 371-7.
31. Vora, B., Khopade, A. J., & Jain, N. K. (1998). Proniosome based transdermal delivery of levonorgestrel for effective contraception. Journal of controlled release, 54(2), 149-165.
32. Dighe SB, Ranawat MS, Raut DN, Jasud SD. Nanotechnology approaches to enhance therapeutic potential of Bacosides and Bacoside rich fractions targeting brain. Journal of medical pharmaceutical and allied sciences. January 2022; 1(2):143-149.
33. Dighe SB , Ranawat MS, Extraction, isolation, characterization and pharmacological evaluation of Bacoside rich fraction from Bacopa monnieri. Afr.J.Bio.Sc. 6(1) (2024), 522-537, ISSN:2663-2187.
34. Thabet, Y., Elsabahy, M., & Eissa, N. G. (2022). Methods for preparation of niosomes: A focus on thin-film hydration method. Methods, 199, 9-15.
35. Goyal, G., Garg, T., Malik, B., Chauhan, G., Rath, G., & Goyal, A. K. (2015). Development and characterization of niosomal gel for topical delivery of benzoyl peroxide. Drug delivery, 22(8), 1027-1042.
36. Kumar, R., & Garg, R. (2020). Formulation and evaluation of solid lipid nanoparticles loaded with bacoside rich extract. Int J Pharm Sci Res, 11(1), 371-7.
37. Patil, S. H., &Janjale, M. V. (2012). Novel and validated titrimetric method for determination of selected angiotensin-II-receptor antagonists in pharmaceutical preparations and its comparison with UV spectrophotometric determination. Journal of pharmaceutical analysis, 2(6), 470-477.

38. Anand, T., Jalarama, R. K., Ramya, S., & Khanum, F. (2018). Optimization of conditions for nanoencapsulation of bacoside rich extract by RSM technique and its characterization. Front Nanosci Nanotechnol, 4, 1-7.
39. Chandira, M., Venkateswarlu, B. S., Shankarrao, J., Bhowmik, D., Jayakar, B., & Narayana, T. V. (2010). Formulation and evaluation of extended release tablets containing metformin HCl. International Journal of chemtech research, 2(2), 1320-1329.
40. Gohel, M., Purohit, A., Patel, A., & Hingorani, L. (2016). Optimization of bacoside a loaded snedds using d-optimal mixture design for enhancement insolubility and bioavailability. International Journal of Pharmacy and Pharmaceutical Sciences, 213-220.
41. Kotha, A. A., Ahmad, S. U., Dewan, I., Bhuiyan, M. A., Rahman, F. I., Naina Mohamed, I., & Reza, M. S. (2023). Metformin hydrochloride loaded mucoadhesive microspheres and nanoparticles for anti-hyperglycemic and anticancer effects using factorial experimental design. Drug Design, Development and Therapy, 3661-3684.
42. Roger, E., Lagarce, F., Garcion, E., & Benoit, J. P. (2010). Biopharmaceutical parameters to consider in order to alter the fate of nanocarriers after oral delivery. Nanomedicine, 5(2), 287-306.
43. Raina, H., Kaur, S., & Jindal, A. B. (2017). Development of efavirenz loaded solid lipid nanoparticles: Risk assessment, quality-by-design (QbD) based optimisation and physicochemical characterisation. Journal of Drug Delivery Science and Technology, 39, 180-191.
44. Gaikwad, D. S., Chougale, R. D., Patil, K. S., Disouza, J. I., &Hajare, A. A. (2023). Design, development, and evaluation of docetaxel-loaded niosomes for the treatment of breast cancer. Future Journal of Pharmaceutical Sciences, 9(1), 43.
45. Moghtaderi M, Mirzaie A, Zabet N, Moammeri A, Mansoori-Kermani A, Akbarzadeh I, Eshrati Yeganeh F, Chitgarzadeh A, Bagheri Kashtali A, Ren Q. Enhanced antibacterial activity of Echinacea angustifolia extract against multidrugresistant Klebsiella pneumoniae through niosome encapsulation. Nanomaterials. 2021 Jun 15;11(6):1573.
46. Zaid Alkilani, A., Hamed, R., Abdo, H., Swellmeen, L., Basheer, H. A., Wahdan, W., & Abu Kwiak, A. D. (2022). Formulation and evaluation of azithromycin-loaded niosomal gel: optimization, in vitro studies, rheological characterization, and cytotoxicity study. ACS omega, 7(44), 39782-39793.
47. Amores, S., Domenech, J., Colom, H., Calpena, A. C., Clares, B., Gimeno, Á., &Lauroba, J. (2014). An improved cryopreservation method for porcine buccal mucosa in ex vivo drug permeation studies using Franz diffusion cells. European Journal of Pharmaceutical Sciences, 60, 49-54.
48. Komada, M., Takao, K., & Miyakawa, T. (2008). Elevated plus maze for mice. Journal of visualized experiments: JoVE, (22).
49. Sireeratawong, S., Jaijoy, K., Khonsung, P., Lertprasertsuk, N., &Ingkaninan, K. (2016). Acute and chronic toxicities of Bacopa monnieri extract in Sprague-Dawley rats. BMC complementary and alternative medicine, 16, 1-10.
50. Vorhees, C. V., & Williams, M. T. (2006). Morris water maze: procedures for assessing spatial and related forms of learning and memory. Nature protocols, 1(2), 848-858.
51. Venkataramaiah, C., Swathi, G., & Rajendra, W. (2018). Morris water maze–a benchmark test for learning and memory disorders in animal models: a review. Asian J Pharm Clin Res, 11(5), 25-29.
52. Hughes, R. N. (2004). The value of spontaneous alternation behavior (SAB) as a test of retention in pharmacological investigations of memory. Neuroscience & Biobehavioral Reviews, 28(5), 497-505.
53. Zhang, Y., Zhu, M., Sun, Y., Tang, B., Zhang, G., An, P.,& Zhou, X. (2021). Environmental noise degrades hippocampus-related learning and memory. Proceedings of the National

Academy of Sciences, 118(1), e2017841117.
54. Hu, L., Tang, X., & Cui, F. (2004). Solid lipid nanoparticles (SLNs) to improve oral bioavailability of poorly soluble drugs. Journal of Pharmacy and Pharmacology, 56(12), 1527-1535.
55. Luo, Y., Chen, D., Ren, L., Zhao, X., & Qin, J. (2006). Solid lipid nanoparticles for enhancing vinpocetine's oral bioavailability. Journal of controlled release, 114(1), 53-59.